

**OCEAN RESOURCES INVESTIGATION
IN THE SEA AREA OF CCOP/SOPAC
REPORT ON THE JOINT BASIC STUDY
FOR THE DEVELOPMENT OF RESOURCES**

(VOLUME 5)

SEA AREA OF REPUBLIC OF KIRIBATI

February 10, 1990

**JAPAN INTERNATIONAL COOPERATION AGENCY
METAL MINING AGENCY OF JAPAN**

MPN
CR(5)
90-23

JICA LIBRARY



1082649(3)

2119}

**OCEAN RESOURCES INVESTIGATION
IN THE SEA AREA OF CCOP/SOPAC
REPORT ON THE JOINT BASIC STUDY
FOR THE DEVELOPMENT OF RESOURCES**

(VOLUME 5)

SEA AREA OF REPUBLIC OF KIRIVATI

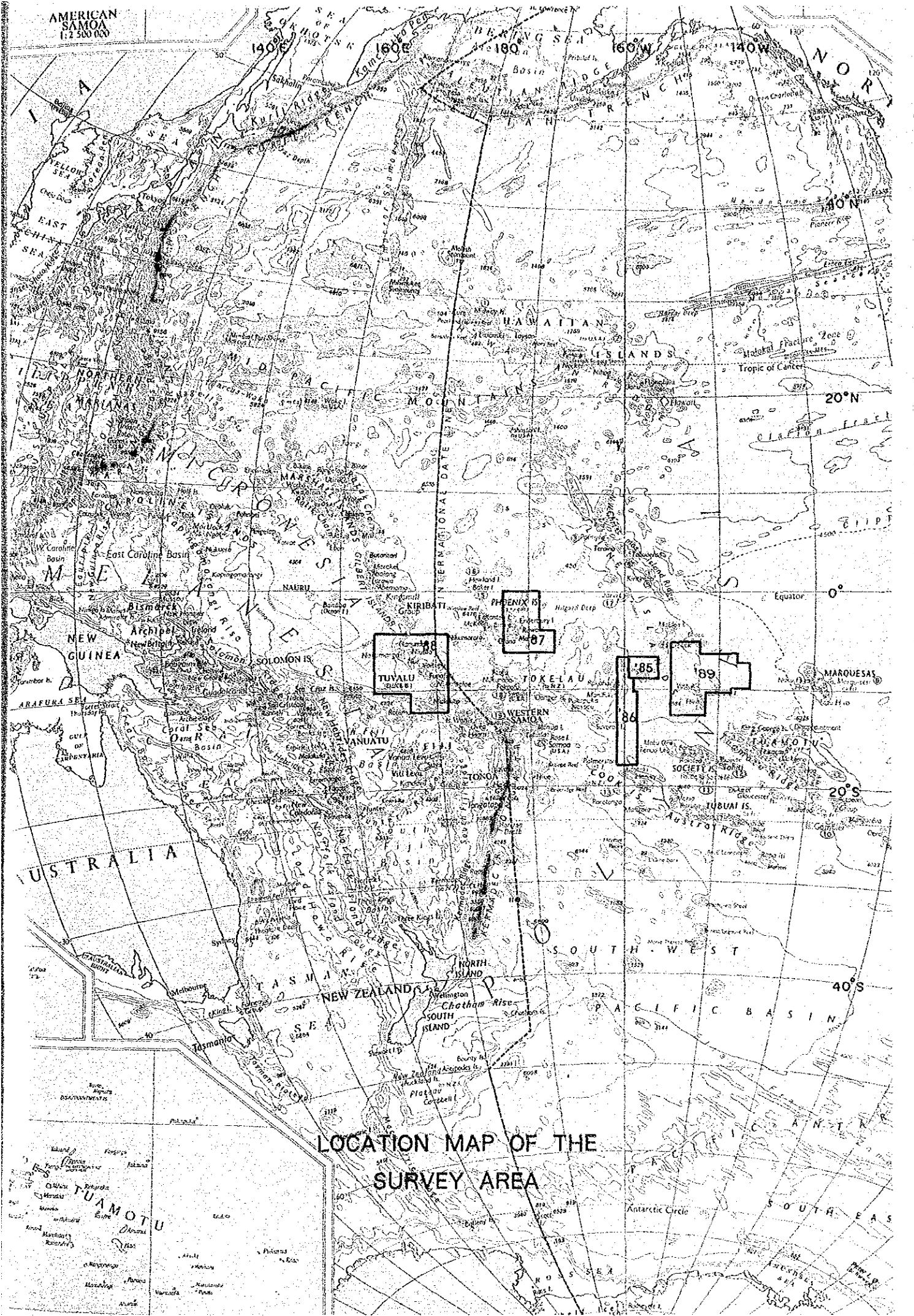
February 10, 1990

**JAPAN INTERNATIONAL COOPERATION AGENCY
METAL MINING AGENCY OF JAPAN**



国際協力事業団

21199



AMERICAN SAMOA
(1:2 500 000)

LOCATION MAP OF THE
SURVEY AREA

TUAMOTU
Arao
Maraa
Kaoi
Manakoa
Raraka
Kaoi
Arao
Maraa
Kaoi
Manakoa
Raraka



89S0947FG03, Abundance 20.90kg/m², Water Depth 4,815m

Sea floor photograph taken by Free Fall Camera. (weight diameter 8 cm)



89SCDC01, Abundance 6.03kg/m², Water Depth 4,818m

Sea floor photograph taken by Continuous Deep Sea Camera (CDC). (weight diameter 10cm)

Representative Occurrence of Manganese Nodule



Sea floor

Slab Type Cobalt Crust

Crust coverage: 88%

Water Depth: 1,403m

SC04 Seamount, FDC03 Track line



Sample collected

Slab Type Cobalt Crust

(Sample No. 89SC02AD02)

Dredged amount: 89kg

Water Depth: 1,810m~1,475m

SC02 Seamount



Section of crust sample

Ditto

(Sample No. 89SC02AD02-B)

Crust thickness: 30~50mm

Substrate: Hyaloclastite

Grade: Co 0.84%

Ni 0.74%

Cu 0.11%

Mn 26.35%

Fe 13.32%

Representative Occurrence of Cobalt Rich Crust

PREFACE

In response to a request by the Committee for Coordination of Joint Prospecting for Mineral Resources in South Pacific Offshore Areas (CCOP/SOPAC), the Government of Japan has undertaken studies relating to mineral prospecting such as marine geological studies to assess mineral resources potential in the deep sea bottom of the offshore regions of the CCOP/ SOPAC member countries. Implementation of the survey has been consigned to the Japan International Cooperation Agency (JICA).

Considering the technical nature of the geological and mineral prospecting studies, the JICA commissioned the Metal Mining Agency of Japan (MMAJ) to execute the survey.

The survey has been undertaken over a five year period starting from the fiscal year of 1985. The subject of the fifth year survey is within the exclusive economic zone of the Republic of Kiribati. The MMAJ dispatched the Hakurei Maru No. 2, a research vessel for investigating mineral resources in the deep sea bottom, to the sites from August 24, 1989 until October 27, 1989, fulfilling the survey on schedule with the cooperation of the Republic of Kiribati.

The present report sums up the results of the fifth year survey.

We wish to extend our sincere thanks to all the persons concerned, especially for the cooperation given to us by the Secretariat of CCOP/SOPAC, the Government of the Republic of Kiribati as well as the Ministry of Foreign Affairs, the Ministry of International Trade and Industry, and the Japanese Embassy in Fiji.

February, 1990

Japan International Cooperation Agency

President Kensuke YANAGIYA

Metal Mining Agency of Japan

President Gen-ichi FUKUHARA

ABSTRACT

The fifth fiscal year fundamental survey for the development of mineral resources in the South Pacific Offshore area (CCOP/SOPAC countries) was carried out in the sea area of the Republic of Kiribati, in an area of approximately 520,000 km². The duration of the survey was from August 28th to October 25th, 1989. The objective minerals of this survey are manganese nodules and cobalt rich crusts (abbreviated as: cobalt crust or crust). Geological and topographical surveys by various acoustic sounding equipment and apparatus were made on manganese nodules. Samplings of manganese nodules and bottom materials at 33 stations were carried out by the free fall grab method at intervals of 60 miles. Sea floor photographs were taken by the continuous photographing deep sea camera (CDC) at favourable zones. The survey on cobalt crusts was made at six seamounts selected as targets. Detailed morphological surveys and dredge-samplings (at 52 points) were carried out at the target seamounts. TV observation and photographing by continuous photographing deep sea camera with finder (FDC) were made at four seamounts to determine minute occurrence of cobalt crusts.

Occurrence of manganese nodules in the whole survey area was not as favorable as expected but comparatively good zones were observed at the eastern sea area. Three seamounts with rich cobalt crusts were confirmed.

The sea floor topography of the survey area is divided by the Line Islands, located in the central part of the sea area and running in the direction of NW-SE, into two parts. The western part is the Plain region of the North Penrhyn Basin with water depths of 5,200 - 5,400 m. The eastern part is the Quasi-plain region of the Northeast Pacific Basin with water depth of 5,000m - 5,200m. The Line Islands line consists of two series in the direction of NW-SE; the western part is composed of knolls and the eastern part of hills. Seamounts SC01-04 belong to the eastern series. Seamount SC05 belongs to the western series and seamount SC06 is in the North Perhyn Basin. Seamount SC05 is a table reef but others are peaked seamounts whose summits are at depths of 805m - 1,590m, deeper to the northward.

The geology of the seamounts is mainly composed of basalt, hyaloclastite, limestone subordinated by pyroclastic rocks, paleo-sediments and unskeletal sediments filling in the crevices. A wide distribution of brown clay is observed in the Plain and Quasi-plain regions, but some parts of them show distributions of calcareous sediments. Based on those distributions the Calcium Carbonate Compensation Depth (CCD) was estimated as approximately 5,000m.

Thickness of unskeletal sediments estimated by SBP is about 10m but, in the aggregate,

the thickness is thin.

(Manganese Nodules)

Average abundance of manganese nodules is as low as 4.37kg/m^2 , but 8% of the whole area has more than 10kg/m^2 . The rich region is located at the Seaknolls of the eastern sea area at depths of 4,700 - 5,100m. Calcareous sediments are distributed in these rich region. Average abundance in the sea area with distribution of calcareous sediments is 7.76kg/m^2 while the area with brown clay is 3.72kg/m^2 . This clearly shows the relation between bottom materials and abundance. Grade average is Ni 0.84%, Cu 0.57%, Co 0.20%, Mn 20.49% and Fe 9.21%. Based on the Mn/Fe ratio, a classification of manganese nodules by grade, Ni-Cu rich types and Co rich types, are identified. Ni-Cu rich types occurred in the plain of Brown clay at places deeper than the CCD and it has low abundance at $\text{Mn/Fe} > 2.5$. While Co rich Type occurs in the Seaknolls of calcareous sediments at around the CCD and it has high abundance at $\text{Mn/Fe} \leq 2.5$.

(Cobalt Crusts)

Seamounts SC01, 02, 06 have excellent grade and thickness of crusts. It is inferable that the seamounts located at the northern part and western part of the Line Islands with older formation age have good conditions of minerals. From the point of morphology, crust type is prominent. High crust coverage on the summit of seamounts, the slopes with irregular exposure rocks and low crust coverage on the plain tops stopping terraces and slumping sediment zones are identified. High Co grade is observed from the substrate of slab type, crust type and hyaloclastite. Distribution of high grade crusts from the summit to the upper part of the slopes in the depth of 1,000 - 1,500m is recognized but a decrease of grade is noticed as the depth increases. The thickness of crusts on sedimentary rocks and pyroclastics substrates is above 27mm while on basalts and limestones it decreases to below 15mm. At depths below 1,500m the thickness is good. Regarding the relation between substrates Ni, Cu, Co grade, a classification of Ni rich group, Co rich group and the medium group was made. Respective substrates of Ni rich crusts, Co rich crusts and the medium group are as follows:

Ni rich crusts : Substrates are Tuff, Tuff Breccia.

Co rich crust : Substrates are Basalt, Hyaloclastite, Limestone.

Medium group : Substrates are Sedimentary rocks such as Sandstone, etc.

This classification is distinctive only in sea areas with shallow depths but in deeper areas types are concentrated in the medium group. Percentage of Cu grade increases as water depth increases and the components approach those of Co rich type manganese nodules.

The occurrences of manganese nodules and cobalt crusts in this sea area are clarified by the survey. In the aggregate, abundance of manganese nodules in this sea area is low but a favourable zone was discovered at the eastern sea area of the Line Islands. On the other hand, three seamounts out of six seamounts are found to be favourable zones. As the detailed occurrences of manganese nodules and cobalt crusts were investigated, we trust that we have obtained a guideline for future surveys.

CONTENTS

	Page
Photogravure	
Preface	
Abstract	
Chapter 1. Main Points of the Survey	1
1-1 Survey Title	1
1-2 Survey Objective	1
1-3 Sea Areas of the Survey	1
1-4 Survey Period	3
1-5 Survey Participants	3
1-6 Survey Apparatus and Equipment	5
1-7 Survey Records	6
Chapter 2. Survey Methods	9
2-1 Manganese Nodules	9
1) Survey Procedures	9
2) Numbering of Track Lines, Sampling Stations and Sampling Points	9
3) Ship Positioning	12
4) Sea Floor Topography	13
5) Surficial Sediments	13
6) MFES Survey of Manganese Nodules	13
7) Sampling and Sea Bottom Observation by Deep Sea Camera	14
8) Observation by CDC	14
9) Processing, Assaying and Storage of Samples	15
10) Processing and Analysis of Survey Data	15
2-2 Cobalt Crusts	20
1) Survey Procedures	20
2) Numbering	21
3) Ship Positioning	21
4) Sea Floor Topography	21
5) Surficial Sediments	21
6) Sampling	22
7) Processing, Assaying and Storage of Samples	22

8) Sea Bottom Observation by FDC	22
9) Processing and Analysis of Survey Data	22
 Chapter 3. Results of Survey 1 (Manganese Nodules)	 24
3-1 Sea Floor Topography	24
1) Regional Topography	24
2) Classification of Sea Floor Topography	24
3-2 Surficial Sediments	27
1) Classification of SBP Records	27
2) Distribution of SBP Types	30
3) Distribution of Upper Transparent Layers	31
3-3 Bottom Materials	32
1) Classification	32
2) Species	32
3) Distribution	33
4) Mineral Composition	36
5) Chemical Composition	40
6) Appraisal of Fossils	40
7) CCD (Calcium Carbonate Compensation Depth)	54
3-4 MFES Survey of Manganese Nodules	55
1) Comparison with Sampling Results	55
2) MFES Estimation of Manganese Nodule Abundance	55
3-5 Modes of Manganese Nodule Occurrence	58
1) Morphology, Size Distribution and Occurrence	58
2) Abundance	64
3) Chemical Composition	69
4) Mineral Composition	89
5) Results of CDC Survey	92
6) Metal Content	97
3-6 Discussions	98
 Chapter 4. Results of the Survey 2 (Cobalt Crusts)	 101
4-1 Seamount Topography	101
1) Classification	102
2) Topographic Features	104
3) Classification by SBP Type	108

4-2	Seamount Geology	110
	1) Geology	110
	2) Description of Substrates	114
	3) Age Determination	125
4-3	Mode of Cobalt Crust Occurrences	126
	1) Type	126
	2) Properties	130
	3) Distribution	133
	4) Chemical Composition	140
	5) Mineral Composition	151
	6) Results of FDC Survey	154
4-4	Discussions	165
Chapter 5. Summary		170
5-1	Survey Methods	170
5-2	Topography and Geology	171
5-3	Mode of Manganese Nodule Occurrence	172
5-4	Mode of Cobalt Crust Occurrence	174

[References]

[Appendix]

1. List of the Survey Results of Manganese Nodules
2. List of the Survey Results of Cobalt Crusts
3. List of the Survey Results by FDC
4. Weather and Sea-state Data

[Annexed Figures]

(List of Inserted Figures)

Figure 1-1	Location Map of the Survey Area	2
Figure 2-1-1	Location Map of Survey Stations and Seamounts	10
Figure 2-1-2	Location Map of Stations	11
Figure 2-1-3	Location Map of Area Codes	11
Figure 2-1-4	Explanation on Setting Order of Three Samplers at Sampling Station	14
Figure 2-1-5	Processing and Assaying Flowsheet of Samples (1), (2)	16
Figure 2-1-6	Data Analysis and Processing Flowsheet	18
Figure 3-1-1	Regional Topography	25
Figure 3-2-1	Classification of SBP Records (1), (2)	28
Figure 3-3-1	Characteristics of Bottom Materials (1)	34
Figure 3-3-2	Characteristics of Bottom Materials (2)	34
Figure 3-3-3	Characteristics of Bottom Materials (3)	35
Figure 3-3-4	Characteristics of Bottom Materials (4)	35
Figure 3-3-5	Typical X-ray Diffraction Patterns of Bottom Materials (1), (2)	38
Figure 3-3-6	Species of the Typical Radiolarian Fossils (1), (2)	44
Figure 3-3-7	Species of the Typical Foraminifera Fossils	52
Figure 3-4-1	Relation between MFES and Sampling Results	57
Figure 3-5-1	Morphology and Sampling Weight of Manganese Nodules	59
Figure 3-5-2	Size and Sampling Weight of Manganese Nodules	60
Figure 3-5-3	Morphology of Manganese Nodules (1), (2), (3)	61
Figure 3-5-4	Photos of Sea Bottom and Samples Collected (1), (2)	65
Figure 3-5-5	Relation between Abundance and Frequency (Sampling Points)	67
Figure 3-5-6	Relation between Abundance and Water Depth (1)	68
Figure 3-5-7	Relation between Abundance and Water Depth (2)	68
Figure 3-5-8	Relation between Bottom Materials and Abundance (1)	70
Figure 3-5-9	Relation between Bottom Materials and Abundance (2)	71
Figure 3-5-10	Morphology and Average Abundance	71
Figure 3-5-11	Frequency Distribution of Five Principal Components	72
Figure 3-5-12	Scatter Distribution Diagrams between Two Components	73

Figure 3-5-13	Abundance-Co Scatter Diagram	75
Figure 3-5-14	Abundance-Ni Scatter Diagram	75
Figure 3-5-15	Triangular Diagram of Ni-Cu-Co by CCD (1)	82
Figure 3-5-16	Triangular Diagram of Ni-Cu-Co by CCD (2)	82
Figure 3-5-17	Relation of Water Depth and (Ni+Cu+Co) Grade	83
Figure 3-5-18	Relation of Mn/Fe and (Ni+Cu+Co) Grade	83
Figure 3-5-19	Triangular Diagram of Ni-Cu-Co by Mn/Fe	84
Figure 3-5-20	Relation of Mn/Fe and Abundance	84
Figure 3-5-21	Distribution Map of Manganese Nodules Mn/Fe	86
Figure 3-5-22	Distribution Map of Manganese Nodules Mn/Fe in the Pacific Ocean	86
Figure 3-5-23	X-ray Diffraction Patterns of Manganese Nodules	90
Figure 3-5-24	Location Map of CDC Trackline (Trackline 89SCDC01)	93
Figure 3-5-25	Variation Charts of Topography, Abundance and Coverage (Trackline 89SCDC01)	94
Figure 3-5-26	Examples of CDC Continuous Photographs	95
Figure 3-5-27	CDC Photographs	96
Figure 3-6-1	Ni-Cu-Co Triangular Diagram (Manganese Nodules)	100
Figure 4-1-1	Established Age Dating of the Line Islands line	101
Figure 4-1-2	Bird's Eye Views of Seamounts	105
Figure 4-1-3	SBP Profile of Seamounts	109
Figure 4-2-1	Photos of Representative Rocks (1), (2)	115
Figure 4-2-2	Microscopic Photos of Substrates (1), (2)	118
Figure 4-2-3	X-ray Diffraction Patterns of Clayish Materials	124
Figure 4-3-1	Occurrence of Cobalt Crust (FDC Photographs)	128
Figure 4-3-2	Representative Cobalt Crust Types (on Board)	129
Figure 4-3-3	Topography of Seamount and Occurrence (SC03 Seamount, FDC Photographs)	131
Figure 4-3-4	Coverage of Cobalt Crust (FDC Photographs)	132
Figure 4-3-5	Characteristics of Cobalt Crust (Surface structure)	134
Figure 4-3-6	Characteristics of Cobalt Crust (Section)	135
Figure 4-3-7	Thickness of Cobalt Crust and Water Depth	136
Figure 4-3-8	Co-Water Depth	144

Figure 4-3-9	Ni-Water Depth	144
Figure 4-3-10	Mn-Water Depth	144
Figure 4-3-11	Fe-Water Depth	144
Figure 4-3-12	Triangular Diagram of Co, Ni, Cu	145
Figure 4-3-13	Triangular Diagram of Co, Ni, Cu	145
Figure 4-3-14	X-ray Diffraction Patterns of Cobalt Crust	153
Figure 4-3-15	FDC Route Map (Line No. 89SC02FDC01) (1)	155
Figure 4-3-15	FDC Route Map (Line No. 89SC03FDC02) (2)	156
Figure 4-3-15	FDC Route Map (Line No. 89SC04FDC03) (3)	157
Figure 4-3-15	FDC Route Map (Line No. 89SC05FDC04) (4)	158
Figure 4-3-16	Examples of FDC Continuous Photographs	159
Figure 4-4-1	General Occurrence of Cobalt Rich Crust	166
Figure 4-4-2	Relation of Co-Ni-Cu Grade and Substrate of Cobalt Crust ...	167

(List of Inserted Tables)

Table 1-1	Survey Apparatus and Equipment	5
Table 1-2	List of Survey Achievements (1), (2)	6
Table 1-3	Records of Survey Schedule	8
Table 3-1-1	Classification of Sea Floor Topography	26
Table 3-3-1	Classification Standard of Bottom Materials	32
Table 3-3-2	Sampling Ratio of Bottom Materials	33
Table 3-3-3	Results of X-ray Diffraction Analysis of Bottom Materials . . .	37
Table 3-3-4	Chemical Composition of the Bottom Materials	41
Table 3-3-5	List of Radiolarian Fossils	43
Table 3-3-6	List of Foraminifera Fossils	51
Table 3-5-1	Chemical Properties of Manganese Nodules	76
Table 3-5-2	Morphology and Chemical Properties of Manganese Nodules	77
Table 3-5-3	Size and Chemical Properties of Manganese Nodules	78
Table 3-5-4	Sea Floor Topography and Chemical Properties of Manganese Nodules	79
Table 3-5-5	Bottom Materials and Chemical Properties of Manganese Nodules	80
Table 3-5-6	Characteristics Classified by Mn/Fe	85
Table 3-5-7	Analysis of Major and Minor Elements of Manganese Nodules	88
Table 3-5-8	Results of X-ray Diffraction Analysis of Manganese Nodules	90
Table 3-5-9	Statistics of CDC Measurements	93
Table 4-1-1	Classification of Seamount Topographic Types	102
Table 4-1-2	Classification of Seamount Topography	102
Table 4-1-3	Area and Average Slope of Each Seamount	103
Table 4-1-4	Topographic Features of Individual Seamounts (1), (2), (3)	106
Table 4-2-1	Geology of Individual Seamounts (1), (2), (3)	111
Table 4-2-2	Results of X-ray Diffraction Analysis of Rocks	117
Table 4-2-3	Results of X-ray Diffraction Analysis of Clayish Materials . . .	123
Table 4-2-4	Results of Chemical Analysis of Clayish Materials	123
Table 4-3-1	Classification of Types of Cobalt Crusts	127

Table 4-3-2	Appearance Rate by Type	130
Table 4-3-3	Thickness of Cobalt Crust (by Type)	137
Table 4-3-4	Thickness of Cobalt Crust (by Substrate)	137
Table 4-3-5	Thickness of Cobalt Crust (by Topography)	137
Table 4-3-6	Thickness of Cobalt Crust (by Depth)	138
Table 4-3-7	Occurrences of Cobalt Crusts at Individual Seamounts (1), (2)	138
Table 4-3-8	Cobalt Crust Grade from Different Layer	141
Table 4-3-9	Correlation Coefficient Table	141
Table 4-3-10	Cobalt Crust Grade and Types	141
Table 4-3-11	Cobalt Crust Grade and Substrates	143
Table 4-3-12	Cobalt Crust Grade and Topographic Position of Seamount ...	143
Table 4-3-13	Cobalt Crust Grade and Water Depth	143
Table 4-3-14	Average Grade of Cobalt Crusts at Each Seamount	146
Table 4-3-15	Analysis of Major and Minor Elements of Cobalt Crusts (1), (2)	149
Table 4-3-16	Correlation Coefficient Table	148
Table 4-3-17	Results of X-ray Diffraction of Cobalt Crust	152
Table 4-3-18	FDC Observation of Cobalt Crust	160
Table 4-3-19	Average Coverage of Cobalt Crust by FDC	163
Table 4-4-1	General Occurrences of Cobalt Crust at Individual Seamount	168

[Appendix]

1. List of the Survey Results of Manganese Nodules
2. List of the Survey Results of Cobalt Crusts
3. List of the Survey Results by FDC
4. Weather and Sea-state Data

[List of Annexed Figures]

- | | |
|-------------------|---|
| Annexed Figure 1 | Trackline Map |
| Annexed Figure 2 | Positions of Sampling Points |
| Annexed Figure 3 | Sea Floor Topography |
| Annexed Figure 4 | Distribution of SBP Types |
| Annexed Figure 5 | Acoustic Thickness of Upper Transparent Layers Obtained by SBP Survey |
| Annexed Figure 6 | Distribution of Bottom Materials |
| Annexed Figure 7 | Estimated Abundance Map of Manganese Nodules by MFES |
| Annexed Figure 8 | Morphology Distribution of Manganese Nodules |
| Annexed Figure 9 | Size Distribution of Manganese Nodules |
| Annexed Figure 10 | Abundance Map of Manganese Nodules |
| Annexed Figure 11 | Ni Grade Map of Manganese Nodules |
| Annexed Figure 12 | Cu Grade Map of Manganese Nodules |
| Annexed Figure 13 | Co Grade Map of Manganese Nodules |
| Annexed Figure 14 | Mn Grade Map of Manganese Nodules |
| Annexed Figure 15 | Fe Grade Map of Manganese Nodules |
| Annexed Figure 16 | Ni Metal Quantity Map |
| Annexed Figure 17 | Cu Metal Quantity Map |
| Annexed Figure 18 | Co Metal Quantity Map |
| Annexed Figure 19 | Trackline Maps of Individual Seamounts (1) ~ (3) |
| Annexed Figure 20 | Topographic Plans and Sections of Individual Seamounts (1) ~ (6) |
| Annexed Figure 21 | Geology and Distribution of Cobalt Crusts of Individual Seamounts (1) ~ (6) |

Chapter 1. Main Points of the Survey

1-1 Survey Title

The 1989 fiscal year Joint Basic Study for the Development of Mineral Resources in the Exclusive Economic Zone of the Republic of Kiribati.

1-2 Survey Objective

The objective of the survey is to assess the potential of deep sea mineral resources, especially that of Manganese Nodules and Cobalt Crusts, in CCOP/SOPAC marine areas. This survey consists of surveys at sea and analysis of data.

1-3 Sea Areas of the Survey

Pursuant to the Cooperative Study Programme relating to deep sea mineral resources in the economic waters of CCOP/SOPAC member countries, concluded on July 17, 1985 between the executing agency of Japan and CCOP/SOPAC, MMAJ designated the marine areas contained in a polygon (area: approximately 519,900 km², Fig. 1-1) bounded by geodesic lines drawn between coordinates listed below:

	Latitude	Longitude
(1)	5°30' S	155°00' W
(2)	5°30' S	152°00' W
(3)	6°30' S	152°00' W
(4)	6°30' S	148°00' W
(5)	7°30' S	148°00' W
(6)	7°30' S	147°00' W
(7)	10°30' S	147°00' W
(8)	10°30' S	149°00' W
(9)	11°00' S	149°00' W

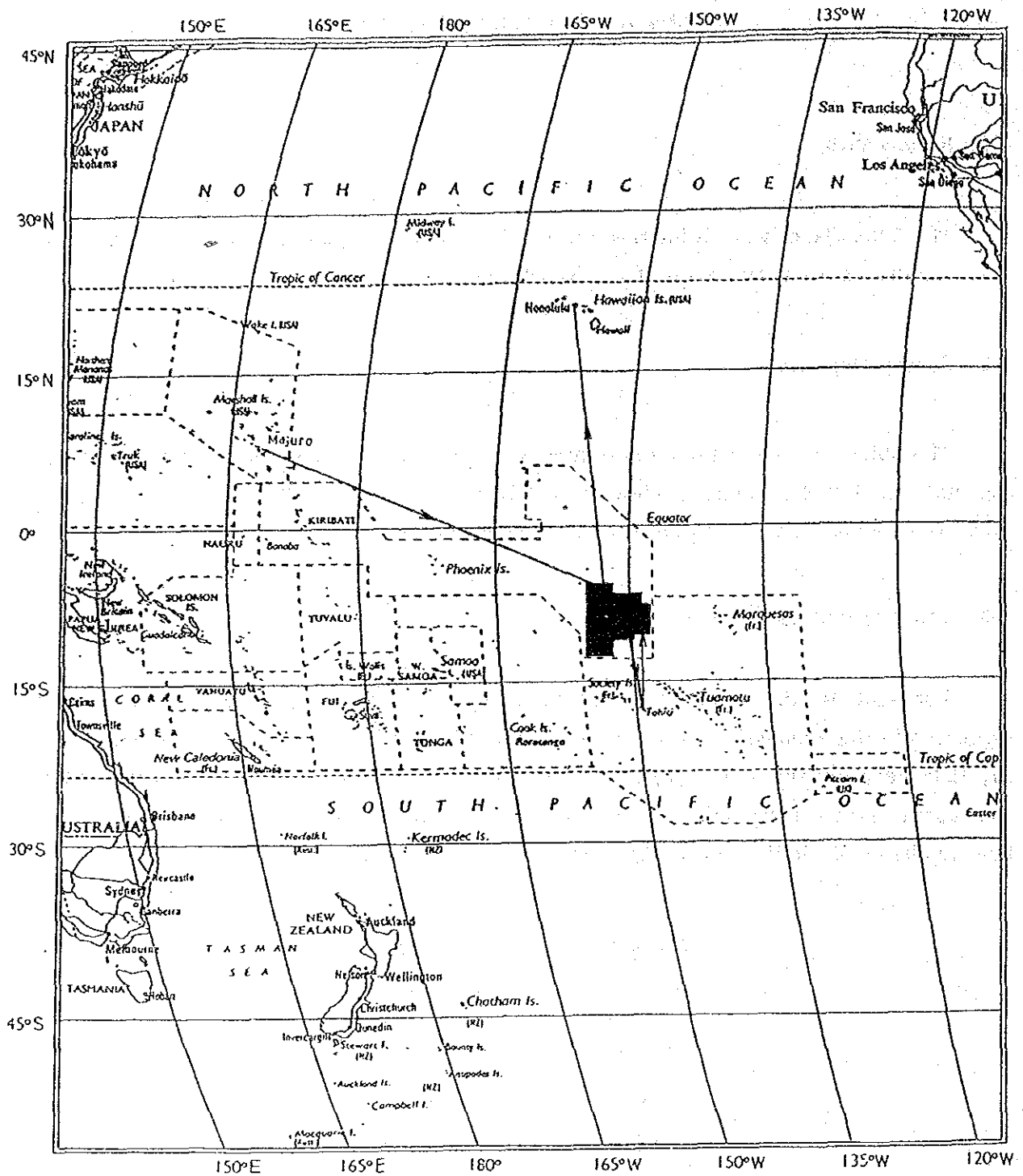


Figure 1-1 Location Map of the Survey Area

(10)	11°00' S	151°30' W
(11)	12°30' S	151°30' W
(12)	12°30' S	155°00' W
(1)	5°30' S	155°00' W

1-4 Survey Period

Survey: August 24, 1989 - October 27, 1989 (65 days)

Analysis: October 28, 1989 - February 10, 1990

1-5 Survey Participants

Japanese Participants

Supervisors at survey sites

Kyoichi KOYAMA	(Metal Mining Agency of Japan)
Katsutoki MATSUMOTO	(")
Seiichi ISHIDA	(")
Etsuo KOZAWA	(")
Nobuyuki MASUDA	(")
Satoshi YAMAGUCHI	(")
Yoshihisa OKUDA	(Geological Survey of Japan, Agency of Industrial Science & Technology)

Members

Team Leader Jiro DATE	(Deep Ocean Resources Development Co., Ltd., DORD)
Chief Geologist Kenji KONAGAI	(DORD)
Geologist Kiyoshi TONO	(DORD)
" Koichi HISATANI	(DORD)
" Yutaka YOSHINAGA	(DORD)
" Yoshikazu YOKOYA	(DORD)
" Takashi MATSUNAGA	(DORD)
" Yuji HANAOKA	(DORD)
" Akihiro TANAKA	(Ocean Engineering and Development Co., Ltd., OED)
Chief Geophysicist Hiroshi MATSUYAMA	(DORD)
Geophysicist Michio TANAHASHI	(DORD)
" Osamu KURAMOTO	(DORD)
" Nadao SAITO	(DORD)
" Seigo KUWABARA	(DORD)
" Terumi YAMAMICHI	(DORD)
" Yoshiki IMAI	(DORD)
" Matsuo IMAI	(OED)
" Toru OHI	(OED)
" Toshiyuki OIKAWA	(OED)

Consigning Participants

Negotiators for the agreement

Jioji KOTOBALAVU	(CCOP/SOPAC)
Jim EADE	(")
C.L.TIFFIN	(")

Advisor

D.S.CRONAN	(")
------------	-------

Participant

Kamatoa BABO	(Republic of Kiribati)
--------------	------------------------

1-6 Survey Apparatus and Equipment

Major apparatus and equipment used during the survey are shown in Table 1-1.

Table 1-1 Survey Apparatus and Equipment

	Survey Method	Survey Apparatus and System	Abbreviation	Remarks
Positioning	Satellite Navigation	Navy Navigation Satellite System	NNSS	
		Global Positioning System	GPS	
Sea Bottom Topography and Geological Survey	Acoustic Sounding Bathymetry Topography	Precision Depth Recorder	PDR	
		Narrow Beam Echo Sounder	NBS	
	Sea Bottom Sound Pressure	Multi Frequency Exploration System	MFES	
	Subsurface Geologic Structure	Sub-Bottom Profiler	SBP	
	Sampling	Free-Fall Grab	FG	
		Spade Corer	SC	
Arm Type Dredger		AD		
Analysis	Pre-Treatment Equipment (Drying-Crushing)			
	X-Ray Fluorescent Analytic Device	XFA		
Sea Bottom Observation	Photograph and TV	Free-Fall Camera	FC	
		Continuous Deep Sea Camera	CDC	Towing Type
		Continuous Deep Sea Camera with Finder *1	FDC	Towing Type
Data Recording and Processing	On Line Functions	Data Processing System	DPS	
	Data Storage Functions	Sensor CPU File Server CPU Host CPU EWS CPU		
	Off Line Functions Track Line Maps Various Plan Maps Cross Sections	LAN ICM PC		

*1 CTD was mounted for bathymetry

1-7 Survey Records

The Survey operations were accomplished as shown in Table 1-2 and Table 1-3.

Table 1-2 List of Survey Achievements (1)

	Item	Accomplishment	
Survey Schedule	Depart Majuro	Aug. 26	16:00
	Arrive in the survey area	Sept. 2	05:30
	Depart survey area	Sept. 15	20:00
	Arrive Papeete, Tahiti	Sept. 17	08:00
	Depart Papeete, Tahiti	Sept. 20	16:00
	Arrive in the survey area	Sept. 22	05:30
	Depart the survey area	Oct. 20	13:30
	Arrive Honolulu	Oct. 26	08:00
Sampling	(Manganese Nodules) Sampling interval Sampling stations Sampling per station Total sampling Samplers used Failure to float	60 mile grid 33 points 3 samples 99 points (33 × 3) Free-Fall Grab (FG): 94 samplings Spade Corer (SC): 5 samplings None	
	(Cobalt Crusts) Number of Seamounts Sampling Stations Samplers Used Amount of Samples Recovered	6 seamounts 52 stations Arm Type Dredge (AD): 52 samplings 2,356 kg (including substrates)	
Deep Sea Observation	(Manganese Nodules) Use of Deep Sea Camera Acquired Photographs Use of Continuous Deep Sea Camera (CDC) Acquired Photographs	99 times 99 188 times 188 (1 track line, 5.4 miles)	
	(Cobalt Crusts) Acquired Photographs (FDC) Acquired VTR Tapes	675 (4 seamounts, 4 track lines, 20.2 miles) 11	
Analysis	Number of Analyses	385 (Manganese Nodules 205) Cobalt Crusts 180)	
	Analyzed Components Total number of Analyzed Components	5 components (Ni, Cu, Co, Mn, Fe) 1,925 (385 × 5 components)	
Acoustic Sounding	(Manganese Nodules) NBS (30.0 KHz) PDR (12.0 KHz) SBP (3.5 KHz) MFES	Length of Traverse	Defective Traverse
	(Cobalt Crusts) NBS (30.0 KHz) PDR (12.0 KHz) SBP (3.5 KHz)	2,580 miles " " " " " " " " 3,633 miles " " " " " "	0 mile " " " " " " " " 0 mile " " " " " "
Data Processing	On Line Sensor MT	14 reels	(Open reel MT)
	On Line FS MT	3 "	(Open reel MT)
	Off Line MT	1 reel	(Open reel MT)
		3 reels	(Cassette MT)

Table 1-2 List of Survey Achievements (2)

	Track Line No.	89SCDC01
CDC	Date	Sept. 24
	Place	Vicinity of Station No. 89426 (W→E)
	Track Line Length (A)	5.4 miles
	Observing Time (hrs.) (T)	05:21
	Average Speed (Kn) (A/T)	1.01
	Equip. Throwing Time	08:26
	Equip. Haul-in Time	16:53
	Survey Duration (hrs.)	08:27
	Number of Photos	188
	Av. Time Interval for each Photo	1.71 min.

	Track Line No.	89SC02 FDC01	89SC03 FDC02	89SC04 FDC03	89SC05 FDC04	Total (Av.)
FDC	Date	Oct. 2	Oct. 4	Oct. 8	Oct. 13	
	Seamount	SC02	SC03	SC04	SC05	
	Track Line Length (miles) (A)	4.1	5.0	6.0	5.1	20.2
	Observing Time (T)	03:00	04:01	04:56	04:47	16:44
	Av. Speed (Kn) (A/T)	1.37	1.24	1.22	1.07	(1.21)
	Equip. Throwing Time	14:31	07:52	07:43	07:42	
	Equip. Haul-in Time	19:01	13:13	14:21	13:58	
	Survey Duration (hrs.)	04:30	05:21	06:38	06:16	22:45
	Number of Photos	137	192	180	166	675
	Av. Time Interval for each Photo (min)	1.31	1.26	1.64	1.73	(1.49)
	Number of Video Tapes	2	3	3	3	11

Table 1-3 Records of Survey Schedule

Duration: 65 days, Survey Duration: 43 days

Month/Day		Survey Items	Month/Day	Survey Items	
8/24	Thu	Preparation for Sailing	9/26	Tue	Co Crust Survey (SC01) ●
25	Fri	◇	27	Wed	◇ ●
26	Sat	Lv. Majuro (16:00)	28	Thu	◇ ●
27	Sun	Training & Meeting	29	Fri	◇ (SC02) ●
28	Mon	Sailing & Preparation	30	Sat	◇ ●
29	Tue	◇ ◇	10/ 1	Sun	◇ ●
30	Wed	◇ ◇	2	Mon	◇ ●
31	Thu	◇ ◇	3	Tue	◇ (SC03) ●
9/ 1	Fri	◇ ◇	4	Wed	◇ ●
2	Sat	Mn Nodule Survey ○	5	Thu	◇ ●
3	Sun	◇ ○	6	Fri	◇ ●
4	Mon	◇ ○	7	Sat	◇ (SC04) ●
5	Tue	◇ ○	8	Sun	◇ ●
6	Wed	◇ ○	9	Mon	◇ ●
7	Thu	◇ ○	10	Tue	◇ ●
8	Fri	◇ ○	11	Wed	Sailing ●
9	Sat	◇ ○	12	Thu	Co Crust Survey (SC05) ●
10	Sun	◇ ○	13	Fri	◇ ●
11	Mon	◇ ○	14	Sat	◇ ●
12	Tue	◇ ○	15	Sun	◇ ●
13	Wed	◇ ○	16	Mon	◇ (SC06) ●
14	Thu	◇ ○	17	Tue	◇ ●
15	Fri	◇ ○	18	Wed	◇ ●
16	Sat	Sailing	19	Thu	◇ ●
17	Sun	Ar. Papeete (08:00)	20	Fri	Survey Completed (13:30)
18	Mon	Off	21	Sat	Drafting Report
19	Tue	◇	22	Sun	◇
20	Wed	Lv. Papeete (16:00)	23	Mon	◇
21	Thu	Sailing	24	Tue	◇
22	Fri	Mn Nodule Survey ○	25	Wed	◇
23	Sat	◇ ○	26	Thu	Ar. Honolulu (08:00)
24	Sun	◇ ○	27	Fri	Handover to succeeding Team
25	Mon	◇ ○			

○: Mn Nodule Survey 18 days

●: Co Crust Survey 24 days

Chapter 2. Survey Methods

2-1 Manganese Nodules

1) Survey Procedures

Zones with water depth suitable for manganese nodule occurrence were selected from the survey area and 33 stations were set. The survey was carried out mainly by free-fall sampling (some by spade corer) and various acoustic soundings at these stations. The CDC (Continuous Deep Sea Camera) survey then proceeded to the stations by selecting one track line from the zone concerned with favourable results. (Fig. 2-1-1)

2) Numbering of Track Lines, Sampling Stations and Sampling Points

(1) Numbering of Track Lines

The track lines for acoustic soundings (NBS, PDR, SBP, MFES) were numbered so that the date and the order of work could be identified by every cruising unit; for instance 89S0902A, 89S0902B. For night cruising, "N" was added to the end of numbers, such as 89S0902N. In these cases, "89" indicates the fiscal year of the survey (1989) and "S" the executing organization (SOPAC): 0902 indicates the month of September and the date of 2nd, and "A, B" the order of track lines on that date.

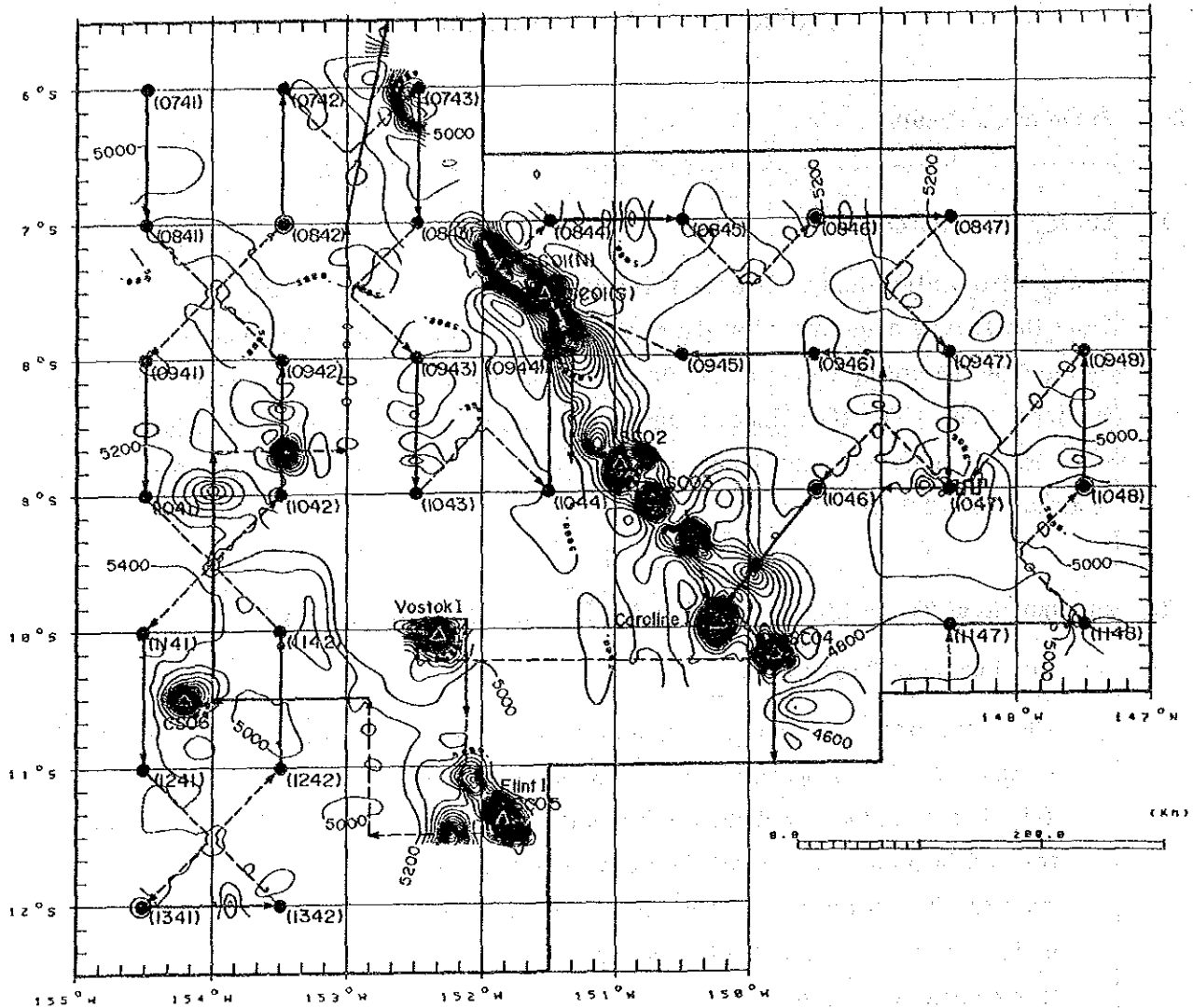
Track lines covered by CDC survey were numbered additionally as 89SCDC01.

(2) Numbering of Stations and Sampling Points

Stations were numbered according to the sampling order, such as 89401. In this case "89" indicates the fiscal year of the survey (1989), "4" the fourth navigation in this year and "01" the sampling order. (Fig. 2-1-2)

To the sampling points, "89S" was prefixed to indicate the fiscal year of the survey (1989) and the executing organization (SOPAC).

The survey area was divided into quadrilaterals by longitudinal and latitudinal lines every 1°. To those quadrilaterals, four-digit area-code numbers were designated as shown in Fig. 2-1-3. In those numbers, the first two figures designate the south side latitudes and the last two figures indicate the longitude, with 175°E designated as (11) and numbers 12, 13, 14...assigned to



LEGEND

- ▭ Survey area
- Sampling station for manganese nodules
- ▲ SC01-SC06 Seamounts for cobalt crust survey
- ⊙ Sampling site by spade corer
- ← Daytime navigation
- ←--- Nighttime navigation
- (0741) Areal block number
- 5,000- Water Depth
- ⋈ FDC survey line
- ⋈ CDC survey line

Figure 2-1-1 Location Map of Survey Stations and Seamounts

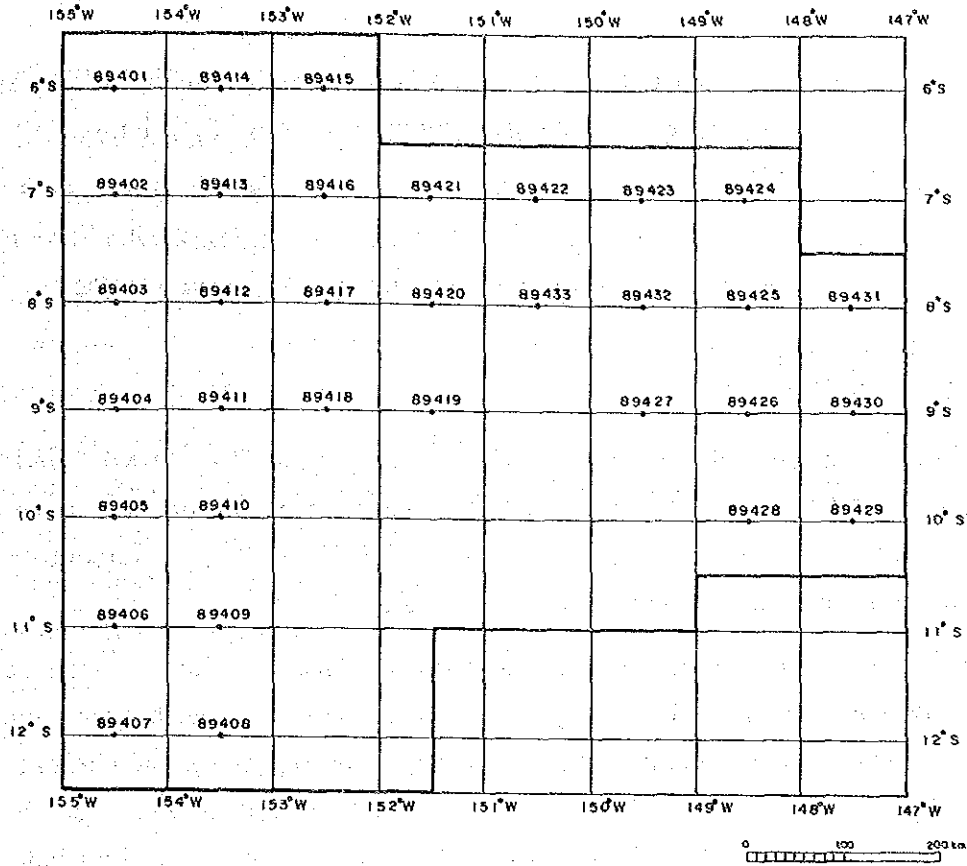


Figure 2-1-2 Location Map of Stations

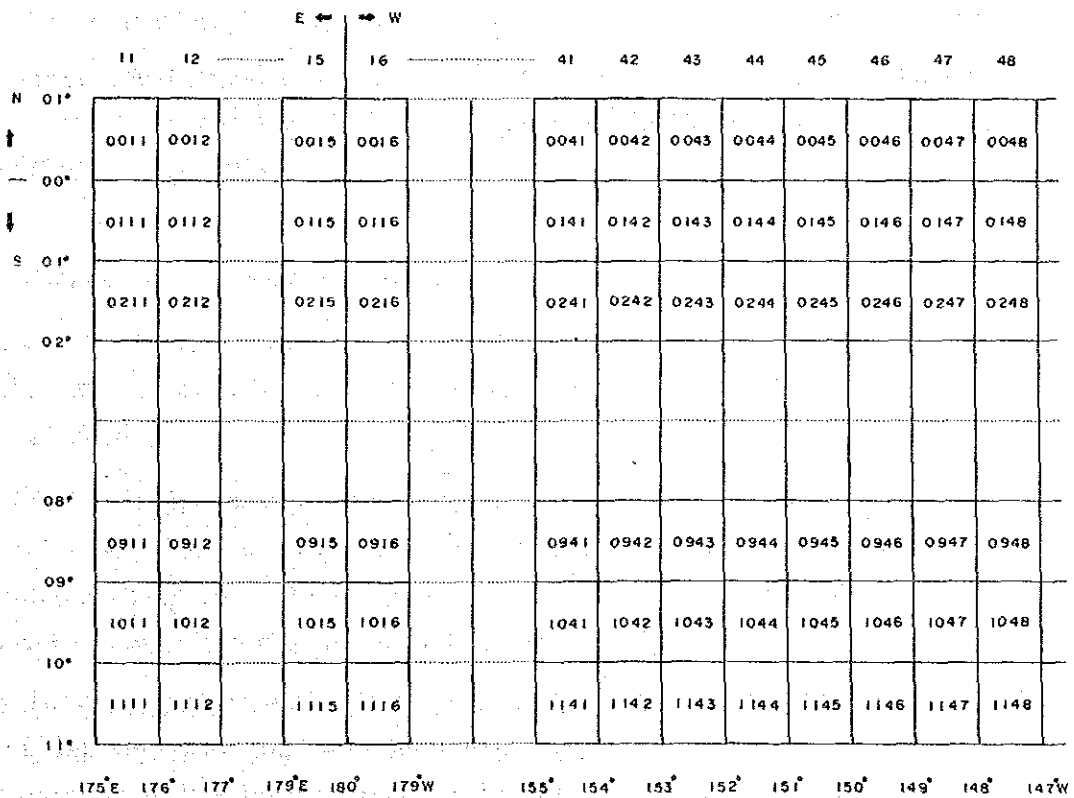


Figure 2-1-3 Location Map of Area Codes

each eastern longitude. The samplings carried out in these areas were numbered with additional figures beginning from "01", indicating respective sampling methods.

Example: The sample number "89S0741FG01" indicates the first (01) sample collected by FG (Free-Fall Grab) in the area 0741SOPAC in 1989.

3) Ship Positioning

During the survey, all the ship positions were indicated by "NNSS" and "GPS". In the case of NNSS, so called "Corrected positions" were used; these were calculated according to the time lag from satellite "Fix Time"*1, to allocate "Fix Data" proportionate to the presumptive navigation positions.

Starting positions, course changes and terminating positions as well as sampler's setting positions and collecting positions were registered with event marks at real time in the data processing system on board so as to process and analyze the survey data. All ship positions relating to the survey activities were registered in the Sensor CPU's MT of the data processing system on board. Also, whenever corrected positions of NNSS were calculated, they were stored in the common file server for constructing a data base and also transmitted to all posts in the vessel through LAN.

At the same time, the corrected vessel positions were printed out by the same system every minute for sorting and analyzing the survey data.

*1 Fix Time: The time when up-dated time and position are determined upon receiving data from a satellite. Ship position will be updated to the real position by this new data.

4) Sea Floor Topography

Depth measurements between the stations as well as between the sampling points were done mainly by NBS, and observations based on the records were also made. (Annexed Figure 1)

Depth sounding was carried out every 12 seconds and the values indicated by NBS digitizer were stored in the common file server and also in the on-line MT. The data stored in the file server was renewed by the pen-touch digitizer before the map of sea-floor topography was drawn by the data processing system. The survey between stations was generally done at 10 knots, but the speed of vessel was changed according to varying conditions. As for the track lines between the sampling points, the speed of the vessel varied in the range of 3-8 knots according to the sampling operation.

5) Surficial Sediments

The survey of the surficial sediments was carried out by SBP (at 3.5 KHz) on all track lines simultaneously with the sea floor topographic survey.

Basic information regarding the surficial sediments consists of data on the thickness of upper transparent layers (based on section pattern records of the SBP), seismic stratigraphic types and so on. This data was read-out every 5 minutes and in-put into the data base of the data processing system. Also, data was plotted on the track map for drawing maps of the Surficial Sediments Isopach and the Distribution of SBP Type.

6) MFES Survey of Manganese Nodules

The distribution density of manganese nodules (Abundance) was surveyed by MFES simultaneously with the survey of the Sea Floor Topography and Surficial Sediments.

MFES data was calculated continuously from sound pressure data of NBS, PDR and SBP every 48 seconds. However, a moving average of 15 measurements was calculated by the data processing system and the results of the said calculation were stored in the file server and the on line MT.

Estimated Abundance Map of Manganese Nodules by MFES was drawn by printing out the MFES off line log list from the data processing system and plotting MFES

values on the trackline map.

7) Sampling and Sea Bottom Observation by Deep Sea Camera

Sampling was carried out mainly by free-fall grab (FG) and partially by spade corer (SC). In addition to the sampling, the sea floor was photographed by deep sea cameras mounted on the samplers. The sampling density of this survey was a 60 mile grid.

At every station, three samplings were done in the following manner. The station was set at the southern apex of a right-angled isosceles triangle with 1.4 miles as the length of the equal sides. Sampling was done at the three apexes of the triangle namely at a distance of 1.4 miles to the northeast and northwest of the station. The order of throw-in of samplers is shown in Figure 2-1-4.

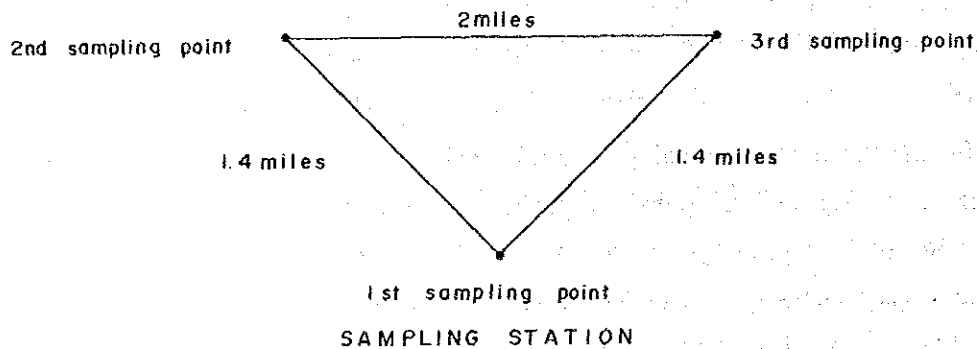


Figure 2-1-4 Explanation on Setting Order of Three Samplers at Sampling Station

When using SC in place of FG, the first of the three samplings, as a rule, was done by SC. In rare cases, when sampling with FG, insufficient sampling due to net damage or incomplete operation is inferred. In such cases, the accuracy of grabbing is calculated by comparing the coverage of the manganese nodules in sea bottom photographs with the samples collected. The grabbing accuracy is used as reference in calculating the abundance.

8) Observation by CDC

The results of sampling at FG 27 stations, which was done during the first half of the survey schedule, showed some favourable manganese nodules. The most favoured station No. 89426 was picked up and a 5 mile west and east track line was

established in the vicinity of the said station. CDC was towed along the track line so as to observe the distribution of manganese nodules.

During the operation of sea bottom observation, vessel speed was kept at about 1 knot and a photograph was taken at every 50 meters.

9) Processing, Assaying and Storage of Samples

The collected samples (manganese nodules and bottom materials) were processed on board, mainly following the processing and assaying flowsheet of FG, SC samples including various measurements and X-ray fluorescence assaying as shown in the Fig. 2-1-5, some of them were also selected for further microscopic observation, X ray diffraction, minor element assaying and so on at the laboratory, the rest kept in storage.

10) Processing and Analysis of Survey Data

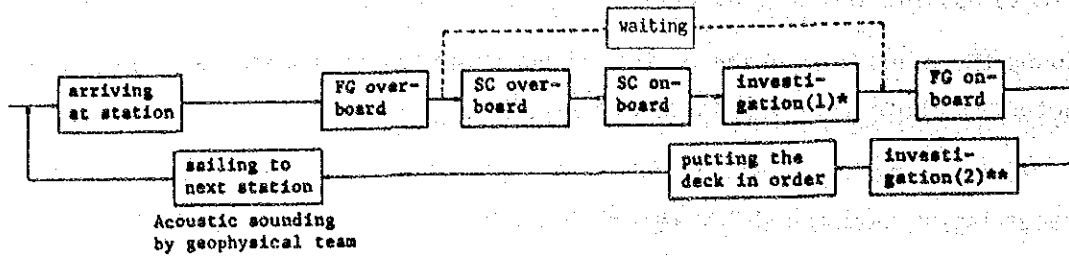
The processing and analysis of the survey data were carried out mainly through on-line functions and off-line functions of the data recording and processing device on board. However, a part of the data processing and comprehensive analysis was done on shore.

A flowsheet of Processing and Analysis is shown in Fig. 2-1-6.

(1) Survey Data and Processing

- ① On-line data from the measuring instruments (such as NNSS, GPS, NBS, PDR, MFES, Winch, Mode Event Box, etc.) was saved in the sensor CPU's MT and also stored temporarily in the buffer. They were processed by computer at the NNSS fix data time and out-put into the common file server according to the prefixed conditions before storing as data base.
- ② From the data of NBS, time and depth were digitized to renew the data stored in the common file server.
- ③ From the data of SBP, Surficial Sediments Data (thickness of the upper transparent layers and stratigraphy type) were read every 5 minutes and in put through OCR so as to store the data in the common file server.
- ④ The survey data on manganese nodules, sediments, assay and others as shown hereunder were registered in the field book for every sampling point. However, a part of them was also stored in the data processing system as sample data.

[A] The outline of the bottom sampling work



* Detail of investigation (1)

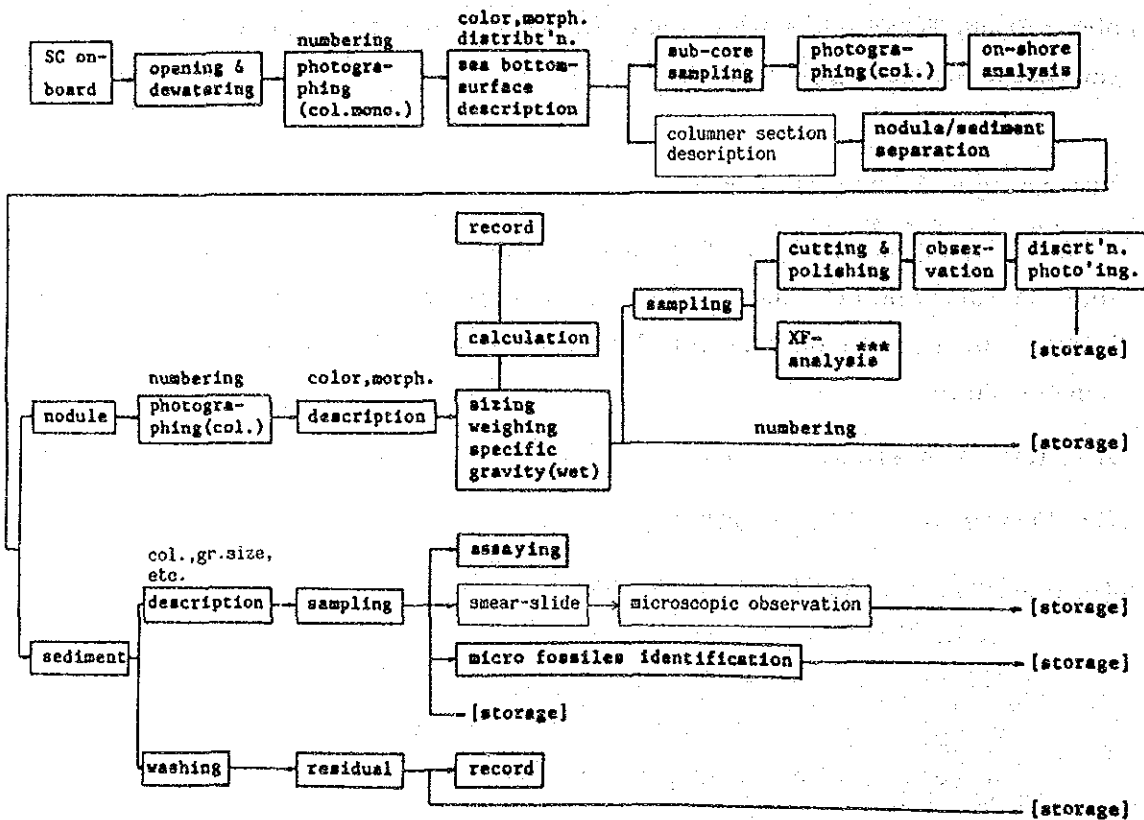
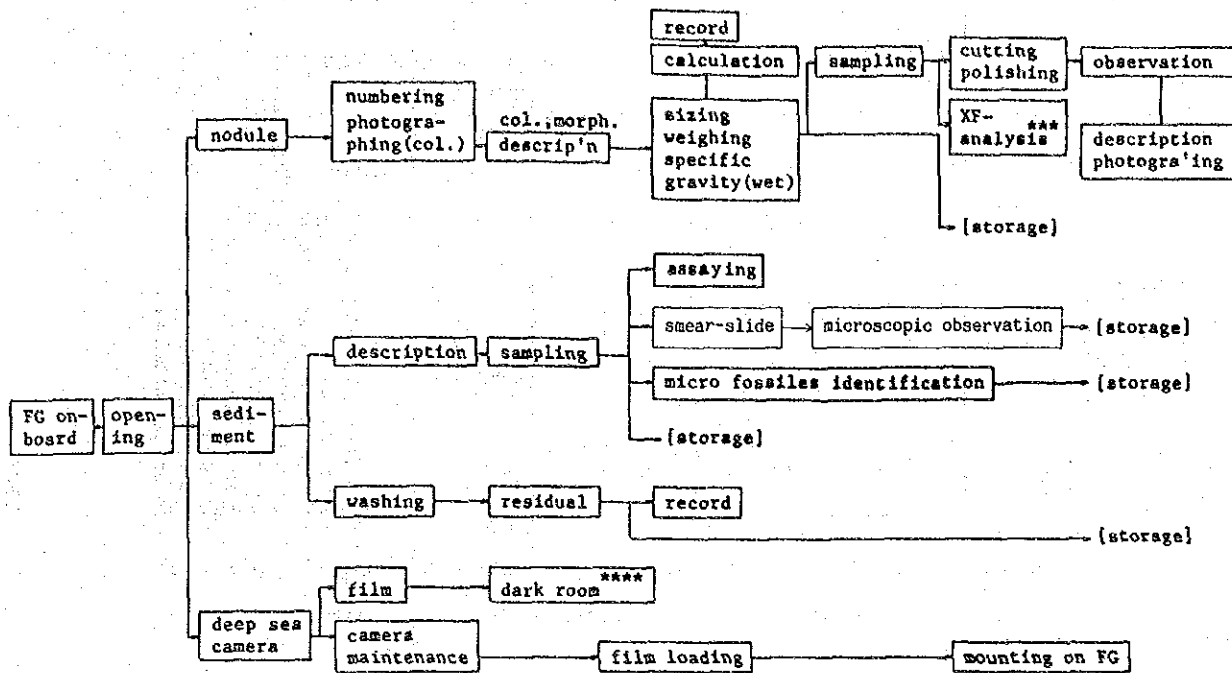
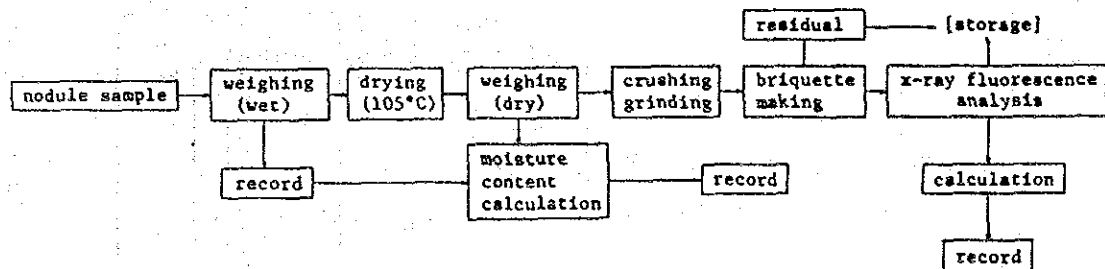


Figure 2-1-5 Processing and Assaying Flowsheet of Samples (1)

** Detail of investigation (2)



*** Detail of XF-analysis



**** Detail of dark room work

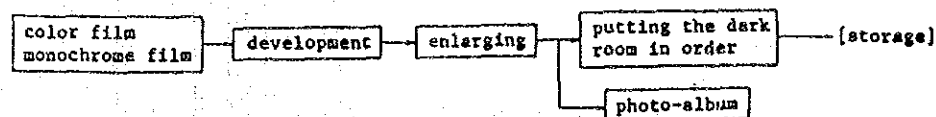


Figure 2-1-5 Processing and Assaying Flowsheet of Samples (2)

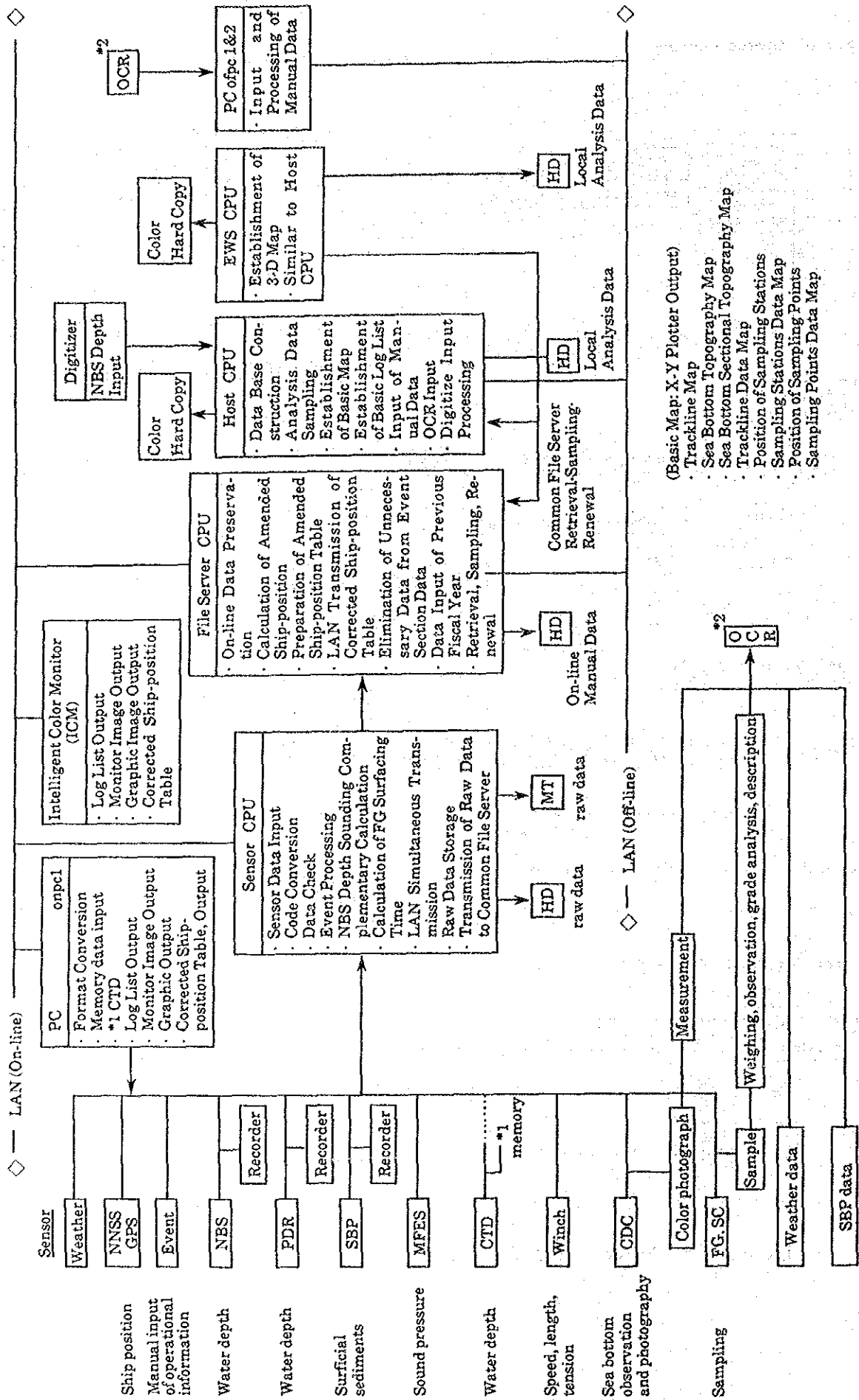


Figure 2-1-6 Data Analysis and Processing Flowsheet

- Data regarding Manganese Nodules: sampled amount, wet weight per grain, apparent specific gravity, shape, number, surface structure, etc.
- Data regarding sediments: type of sediment, colour tone, micro fossils, etc.
- Data regarding assay: grade of 5 principal components (Ni, Cu, Co, Mn, Fe) and water content.
- Photographs on bottom and on board taken by camera mounted in FG, SC
- Acoustic records (NBS records, SBP records)

(2) Analysis of the Survey Data

Following Maps and Tables were made using the data stored in the data processing system and the off line personal computer.

① Trackline Map and Positions of Sampling Points

The Trackline Map and Positions of Sampling Points were plotted on a 1/1,200,000 scale by the off line plotter of the data processing system.

② Sea Floor Topographic Map

Using the bathymetric charts obtained by plotting depth values every 5 minutes on the above mentioned trackline map, the Sea Floor Topographic Maps were drawn with contour intervals of 200 m.

③ Acoustic Thickness Map of Upper Transparent Layers Obtained by SBP Survey

The thickness of upper transparent layers was read out every 5 minutes from SBP records and plotted on the above mentioned trackline maps. Then the isopach maps were completed with contour intervals of 10 m.

④ Distribution Chart of SBP Types

SBP Type Chart was drawn by reading out SBP types every 5 minutes from the SBP record and plotting on the Trackline Map.

⑤ Estimated Abundance Map of Manganese Nodules by MFES

This map was drawn by printing out the MFES log list through off line functions of the data processing system and plotting density values every 5

minutes on the above mentioned Trackline Map. Abundance contours were drawn with intervals of 2kg/m².

⑥ Bottom Materials Chart

The bottom materials chart was made by plotting the classified bottom materials collected by samplers and the quantity of authigenic minerals on the map of sampling point positions.

⑦ Abundance Map of Manganese Nodules, Grade Map and Metal Quantity Map

On the basis of data obtained on manganese nodules at each sampling point (throw-in point of FG, SC, etc.), the average state of ore (abundance, grade, etc.) was calculated for each station (3 samples per station). By working up these results, the Abundance Map of Manganese Nodules, the Grade Map of Nickel, Copper, Cobalt, Manganese and Iron as well as the Metal Quantity Map were made.

The acoustic sounding data, etc. was also referred to in this process.

⑧ Data List

In order to facilitate searching and referencing of the data on the manganese nodules, essential items were excerpted from the field notes and annexed under the title of Data List.

2-2 Cobalt Crusts

1) Survey Procedures

Six seamounts were selected for survey, based on previously known sea floor topographical data and that of newly obtained from the survey of manganese nodules. (Fig. 3-1-1)

The survey mainly consisted of investigating seamount topography and surficial sediments by acoustic soundings, of observing and photographing by FDC and of sampling by dredges.

2) Numbering

Numbering was done as follows;

(Seamounts) S (SOPAC)--Area (this fiscal year represented in alphabetical order of C, and D, E... will be applied successively to other areas from the next fiscal year)-- Number.

Example: SC01.

(Sampling points)

Year--seamount--type of device used--Number

Example: 89SC01AD01

(FDC Track lines)

Year--seamount--FDC--Number

Example: 89SC01FDC01

(Acoustic Sounding Tracklines)

Year--S(SOPAC)--date--N(night)

Example: 89S0927N

(Apparatus and Equipment used in the survey)

Shown in Table 1-1

3) Ship Positioning

The ship positioning used was the same as that for survey of manganese nodules.

4) Sea Floor Topography

Sea floor topography was obtained by NBS topographical sailing at the beginning of each survey. A sea floor topography map was also drawn by the data processing system and sampling points were designated. The designated standard distance between the track lines was 1 mile and the ship speed 10 knots.

5) Surficial Sediments

The distribution of surficial sediments on the seamounts was obtained by means of SBP. The data was subsequently used for selecting the sampling points.

6) Sampling

Sampling was carried out by Arm Type Dredge (AD) on all six seamounts. Target areas were the tops and slopes of the seamounts down to the depth of around 3,100 m. Sampling was done at approximately 9 points on each seamount. The ship speed during dredging was about 1 knot. The standard towing time between the dredges on and off bottom was approximately 30 minutes.

7) Processing, Assaying and Storage of Samples

The dredged samples were weighed and described after being classified into several types on board. A part of every sample was assayed for five components; Co, Ni, Cu, Mn, Fe, and for water content. The method of assay was the same as for the manganese nodules, however, tests for deviation of data (bias tests) were made on the same samples on shore. Microscopic observation, X-ray diffraction, total assay, micro-assay, etc., were carried out on shore as in the case of manganese nodules. As residual samples, some typical ones were stored in water-tight plastic bottles, and the rest were stored wet.

8) Sea Bottom Observation by FDC

Survey by FDC was carried out before sampling in order to observe the mode of occurrence and to photograph typical occurrences of cobalt crusts.

The designated length of track lines was 5 miles, and the standard towing speed was 1 knot during the observation. In principle, the observation were done continuously along the sea bottom. Photos were taken when suitable. A TV camera with finder was loaded on the FDC vehicle, so that both real time observation through monitor TV and detailed observation by VTR was possible. The mode of occurrence of cobalt crusts, especially coverage and lateral variation of crusts which could not be obtained by sampling alone, were recorded by the VTR images and photographs.

9) Processing and Analysis of Survey Data

(1) Survey Data and Processing

Survey data and processing procedures were basically the same as for manganese nodules. However, MFES was not used in the cobalt crust survey, and AD and FDC were used instead of FG, SC and CDC.

Processing flowsheet is shown in Fig. 2-1-6.

(2) Analysis of the Survey Data

Following charts and tables were created using the data processing system or off line personal computer.

① Trackline map

Trackline maps for each seamount were drawn at the scale of 1/300,000 by data processing system.

② Map of sea floor topography and positions of sampling points

Sea floor topography was drawn at 1/300,000 scale for each seamount by data processing system and sampling points were then plotted on it.

③ Cross sections of sea floor topography

Cross sections of seamounts were drawn by the data processing system.

④ Bird's eye view topographical map

A bird's eye view map was drawn for each seamount by the data processing system.

⑤ Slope maps

A slope map for each seamount was drawn by the data processing system.

⑥ Geological sea floor maps and distribution maps of cobalt crusts

Essential points of dredge sampling data and FDC survey data for each seamount were indicated on the sea floor topographical map. The average grade of each sampling was also shown on the map.

⑦ FDC observation survey maps

The mode of occurrence of cobalt crusts obtained from observation of TV images and photo analysis, FDC track lines, cross sections of topography and the estimated coverage of cobalt crust were shown as route maps.

⑧ Various maps showing relevant features were prepared in order to study the resource potential of cobalt crusts.

Chapter 3. Results of Survey 1 (Manganese Nodules)

3-1 Sea Floor Topography

1) Regional Topography (Fig. 3-1-1 and Annexed Fig. 3)

The survey area covers an area where the Line Islands are sandwiched between the eastern part of the North Penrhyn Basin and the Northeast Pacific Basin. The water depth of the southwestern part, which belongs to the North Penrhyn Basin, is 5,200~5,400m, with the formation of deep-sea plain.

The northeastern part of the survey area belongs to the Northeast Pacific Basin and its water depth is also around 5,000~5,200m. These two sea-basins are divided by the Line Islands which run in the central part of the survey area in a northwest-to-southeast direction.

The central part of the sea area is located at the end of the northern part of the Line Islands line which composes Christmas Island Ridge up to the west of Hawaii Island and is known as the Southern Line Group. This Line Islands line consists two parallel series in the sea area; one is Caroline Island which belongs to the eastern line, the other is Vostok Island and Flint Island which belong to the western line. Most of the seamounts of which the Line Islands line is composed are made up of independent small-scale peaked seamounts. However, the northern portion of the eastern seamounts is made up of continuous ridges.

Topographic features of individual seamounts are described in the chapter of Cobalt Rich Crust.

2) Classification of Sea Floor Topography

In order to grasp characteristics of the entire area, the sea floor topography is classified in two ways: from the macro-topographic point of view (macro classification) and from the micro-topographic point of view (micro classification).

Definitions of topographical classifications are shown in Table 3-1-1.

From the viewpoint of macro sea floor topography, the present survey area can be classified into Plain, Hill, Mountainous and Quasi-plain zones running from west to east in the order named above. Among them, the Mountainous and Hill zones correspond to the Line Islands line which crosses the central part of the surveyed area in the NW-SE direction. The Line Islands line in this surveyed area is

composed of two parallel series: the western line corresponds to the Hill zone and the eastern one corresponds to the Mountainous zone.

The Plain zone corresponds to the eastern part of the North Penrhyn Basin. The Quasi-plains are facing the area where the Northeast Pacific Basin touches the Line Islands line.

From the viewpoint of micro sea floor topography, the surveyed area can be classified into Flat, Hollow, Channel, Platform, Sea knoll, Seamount and Ridge areas.

Among them, Flats are widely distributed in the Plains, Hills and Quasi-plains.

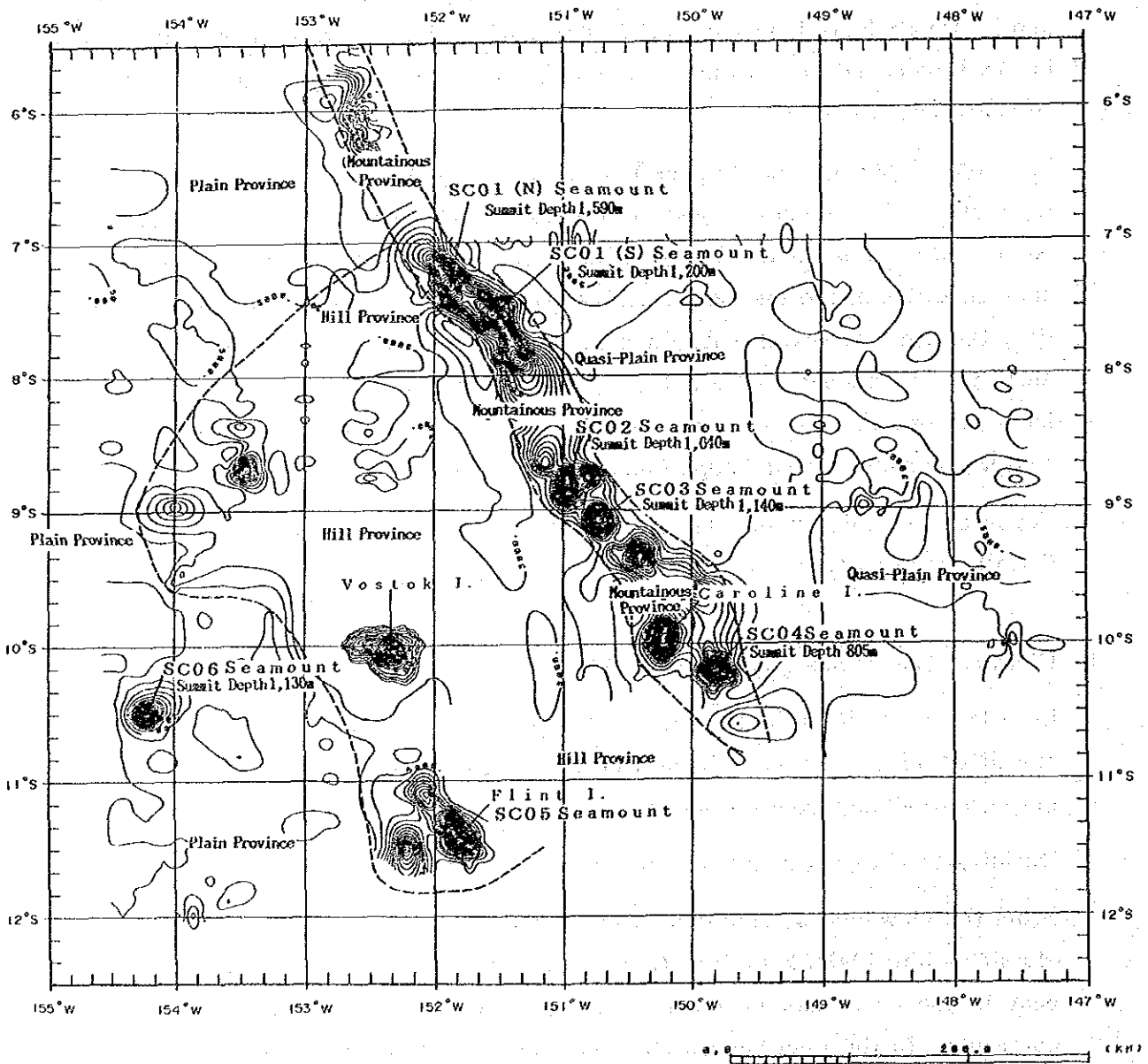


Figure 3-1-1 Regional Topography

There are comparatively large-scaled Hollows in the North Penrhyn Basin located at the western part of the surveyed area and in the Northeast Pacific Basin located at the northeastern part of the surveyed area. Also, a Hollow of 5,200~5,400m, is recognized at the northern part of the Line Islands line.

Channels are recognized around the northern part of the Line Islands line with some dents reaching to the depth of 5,800m.

Small-scaled Platforms are recognized in the Hill and the Quasi-plain zones.

Sea knolls are found in the Hill and the Quasi-plain zones, but are very few in number, and the relation with the Line Islands line is not indicated.

Small-scale Seamounts are distributed throughout the Line Islands line Area. Only one Seamount is recognized, exceptionally in the North Penrhyn Basin (SC06).

There is a Sea knoll (SC01) about 150 km long at the northern part of the Line Islands line.

Table 3-1-1 Classification of Sea Floor Topography

Topographical classification		Definition
Regional province	Plain	Area where the sea floor is almost flat and with isolated seamounts or sea knolls, it may be considered as plain from a general point of view.
	Hill	Area where numerous sea knolls or seamounts are dispersed.
	Mountainous	Area where the outstanding mounts or knolls are usually observed.
	Quasi-plain	Area where the bottom is rather undulated and which can be classified neither as plain nor as hilly.
Local area	Flat	Plain area not undulated or smoothly undulated (up to about 100 m relative height) and which does not belong to the hollow or the platform.
	Hollow	Area with smooth undulation and which presents a generally concave terrain, including a ship-shaped basin.
	Channel	Long and narrow concave terrain in a ditch shape, including fissures or fracture zones.
	Platform	Area with smooth undulation which presents as a whole a convex terrain (or a tableland).
	Sea knoll	Hilly area with a relative height of less than about 1,000 m, including entire slope as well as summit.
	Seamount	Hilly area with a relative height of more than about 1,000 m, including entire slope as well as summit (the sloping surface contains a shifting part of the plain).
	Ridge	Terrain presenting a chain of mountains composed of the sea knolls and hills ranged in a zone.
	Other	Terrain not belonging to any of the above mentioned classifications.

3-2 Surficial Sediments

1) Classification of SBP Records

The SBP Types found in this surveyed area are classified into 2 groups. The one group is in which the transparent layers are recognized in the upper layer: type a, type b, type e₁, type t_s. The other group is in which the acoustic opaque layers are recognized in the upper layer: type c, type d₁, type d₂ and type d_s. Typical examples of each type are shown in Fig. 3-2-1.

Definitions of each type are as follows :

① Types in which the acoustic transparent layers are recognized in the upper layers.

Type a: Composed of two layers, transparent and opaque; the transparency of the transparent layer is high, with a clear border line between the transparent layer and the opaque layer.

Thickness of the transparent layer is 20~30m.

Topography is Plain.

Type b: Composed of two layers, transparent and opaque; the transparency of the transparent layer is not as high as type a, and the border with the opaque layer is obscure.

Thickness of the transparent layer is 30~50m.

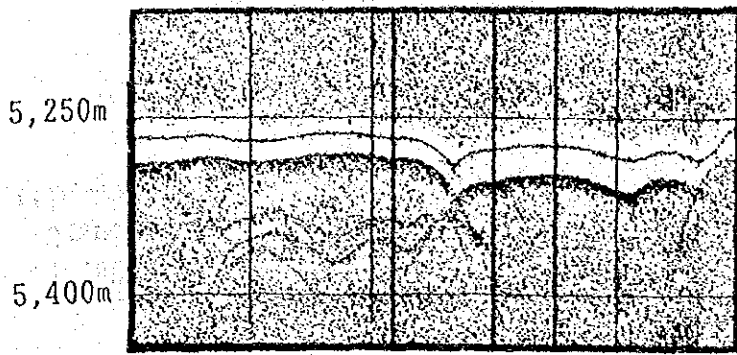
Type e₁: Normally composed of two layers, transparent and opaque, but portions have multistratified structure. Although the transparency of the transparent is lower than that of type a, it shows a clear border with the opaque layer. Distributed in the Hill zone.

Thickness of the transparent layer is 10~20m.

Type t_s: Various hyperbolic curves caused by the topography are recognized. The transparency of the upper layer is comparatively high. Existence of transparent layer is inferred.

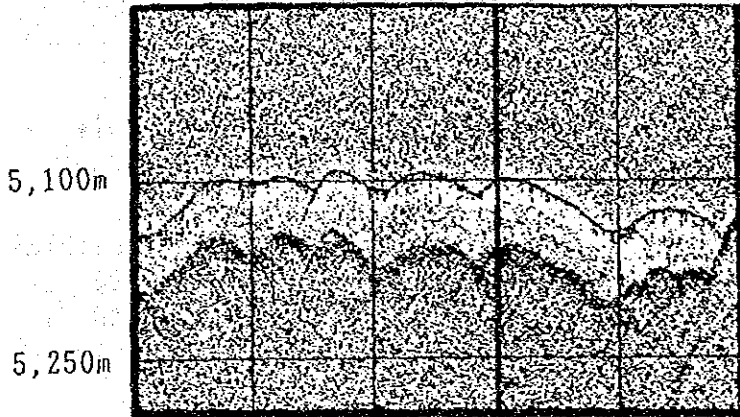
Distribution of pre-congealed sediments on the upper layer is inferable with above mentioned types.

Generally, manganese nodules occur in the areas with sediments of type a, but no such tendency is recognized in this sea area.



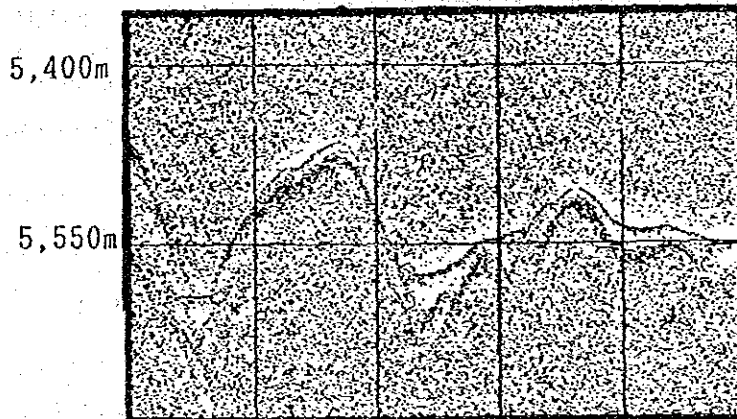
Type a

Line 89S0905
 12° 00' S
 153° 30' W



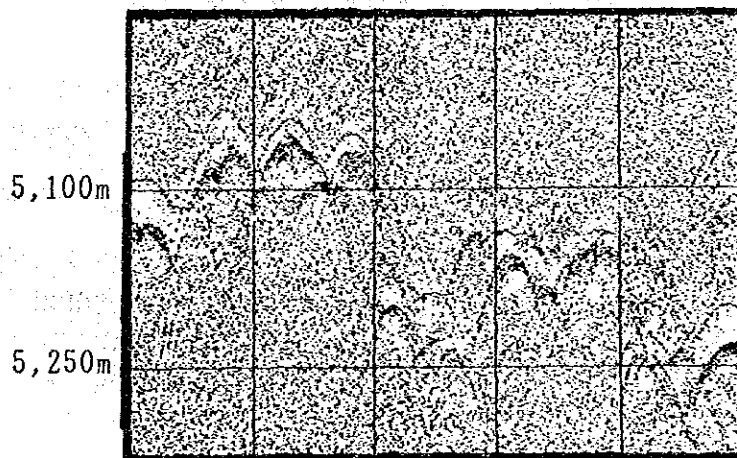
Type b

Line 89S0908N
 06° 00' S
 153° 30' W



Type e₁

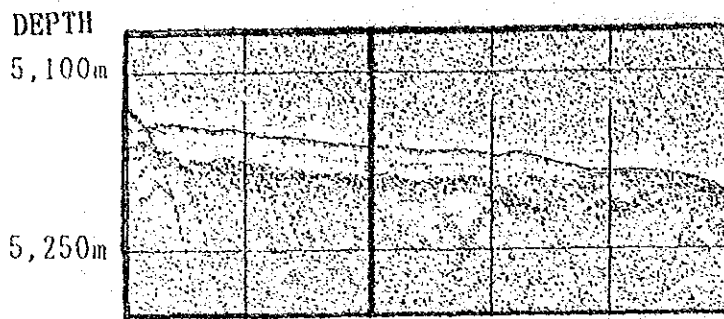
Line 89S0903N
 09° 49' S
 154° 19' W



Type t_s

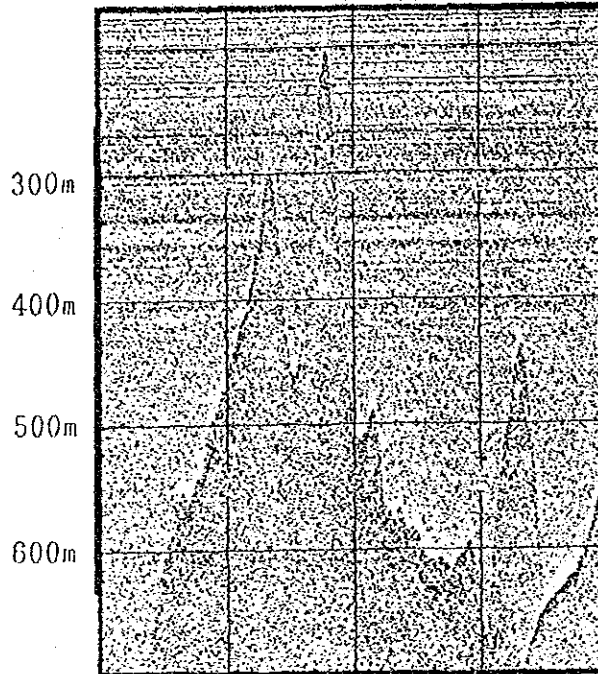
Line 89S0913N
 07° 00' S
 148° 30' W

Figure 3-2-1 Classification of SBP Records (1)



Type c

Line 89S0911A
 08° 10' S
 151° 30' W



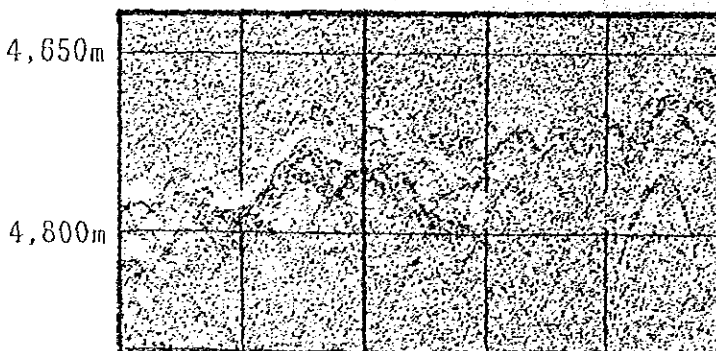
Type d1

Line 89S1012A
 11° 24' S
 151° 49' W



Type d2

Line 89S0909A
 06° 24' S
 152° 30' W



Type ds

Line 89S0922
 10° 19' S
 148° 30' W

Figure 3-2-1 Classification of SBP Records (2)

② Types in which the acoustic opaque layers are recognized among the upper layers:

Type c: Many cases show alternations of opaque and transparent layers. Alternation of congealed sediments on the upper layers and pre-congealed sediments in the lower layers are inferable.

Type d₁: Composed of opaque layers only. This type is generally found at Seamounts, Sea knolls, etc., and most of these zones correspond to the exposed basement rocks.

Type d₂: Composed only of opaque layers, and mainly observed in Plains. Distribution of basement rocks or congealed sediments are inferred.

Type d₃: Various hyperbolic curves caused by the topography are recognized. The transparency of the upper layers is low and the existence of opaque layers is inferred. These provinces correspond to the exposed rocks and comparatively congealed sediments.

2) Distribution of SBP Types

Distribution of SBP Types is shown in Annexed Figure 4. This surveyed area can be classified into four zones are previously stated:

Plain : West of 153°W, Water depth; 5,000~5,400m.

Quasi-plain : At the northeastern part of the surveyed area. Water depth; 5,000~5,200m.

Hill : Roughly in the central part of the surveyed area. Water depth; 4,500~5,000m.

Mountainous : Distributed in the NW-SE direction of the central part of the surveyed area.

Distribution of SBP Types in this sea area indicates close relation with the topography.

Followings are characteristics of SBP Types;

① Plain : Transparent layers of type e₁, a, b, are mainly found in the Plains. Type e₁ is widely developed in the southeastern part of the sea area. Types e₁ and b are prominent at the northwestern part of the sea area. Type c is widely

distributed in the area between 7°S and 9°S. Type a and type ts are found locally.

- ② Quasi-plain : Type ds is prominently recognized. Other types are found only locally.
- ③ Hill : Type ds is widely developed, other types are recognized locally. Type c is prominent around the Mountainous zone.
- ④ Mountainous : Type d₁ and type ds are widely developed.

Type ds is widely distributed in the zones other than the Plains. About 80% of the sea area is occupied by the Quasi-plain, Hill and Mountainous zones. Consequently, about 80% of the sea area has type ds. In the Flat region, type d_s is considered to correspond to the type d₂ or the type c, and the distribution of comparatively high-congealed sediments is inferred. Particularly at depths shallower than the CCD (about 5,000m) the zones correspond to the distribution of calcareous sediments.

3) Distribution of Upper Transparent Layers

Annexed Figure 5 shows the distribution of upper transparent layers. As previously stated, opaque layers represented by the type ds are scattered widely in the survey area, so the area of the transparent layers is extremely limited. The transparent layers of type e₁ and type b occur in limited zones in the southwestern and north-western parts of the survey area. The thickness of the transparent layers in those zones is about 10m, but occurred in comparatively sizable regions. Topographically, they are located at the water depths of 5,000~5,400m, and correspond to the deep sea Flat zone of the North Penrhyn Basin. At other regions, transparent layers corresponding to the types a, b, e₁ and ts with the thickness from 10m to 30m are recognized, but lacking in continuity.

3-3 Bottom Materials

1) Classification

Bottom materials are classified according to the criteria shown in Table 3-3-1. Quantitative analysis of each composition was made by microscopic observation using smear slides ($\times 100$).

Table 3-3-1 Classification Standard of Bottom Materials

	Total Fossil (%)	Siliceous *1 Fossil (%)	Calcareous *2 Fossil (%)	Remarks
Brown clay	< 10			
Siliceous clay	10 ~ 30		< 5	
Silic-calcareous clay	10 ~ 30		> 5	Siliceous fossil > Calcareous fossil
Calc-siliceous clay	10 ~ 30	> 5		Calcareous fossil > Siliceous fossil
Calcareous clay	10 ~ 30	< 5		
Foraminifera ooze	> 30			Mainly foraminifera
Silic-calcareous ooze	> 30		> 5	Siliceous fossil > Calcareous fossil

*1 Radiolaria, Diatom, Silicoflagellate, Sponge spicule

*2 Foraminifera, calcareous nannoplankton

2) Species

The species and the sampling ratio of bottom materials collected at 84 points out of 99 FG and SC sampling points is shown in Table 3-3-2.

Table 3-3-2 Sampling Ratio of Bottom Materials

Age	Species	Sampling Numbers	Ratio (%)	
Quaternary	Brown clay	63	75.0	100
	Siliceous clay	1	1.2	
	Calcareous Sediments			
	a. Calc-siliceous clay	7	8.3	
	b. Silic-calcareous clay	9	10.7	
	c. Calcareous clay	1	1.2	
	d. Silic-calcareous ooze	1	1.2	
e. Foraminifera ooze	2	2.4		

Following features are observed;

- ① Only Quaternary sediments are observed.
- ② Rich in calcareous sediments. (about 24%)

Calcareous sediments are predominantly observed in the eastern sea area off the Line Islands. This reflects the fact that many sampling points are located at depths of less than 5,000m.

	<u>Western area</u>	<u>Eastern area</u>
Calcareous sediments	19%	32%

- ③ Most of the Brown clay is the color of 5YR2.5/2, dark reddish brown.
- ④ Some Brown clay contains high content of zeolite, marking as much as 10%.

3) Distribution

Characteristics of the sediments in the survey area are as follows;

- ① Brown clay appears throughout the whole area. (Annexed Figure 6)
- ② To the west of the Line Islands, calcareous clay appears on the shallow part of the seamounts.
To the east of the Line Islands, it appears in the shallow parts of 9°S. (Annexed Figure 6)
- ③ Fluctuation of Radiolaria content in Brown clay is observed. (Figure 3-3-1 to Figure 3-3-4).

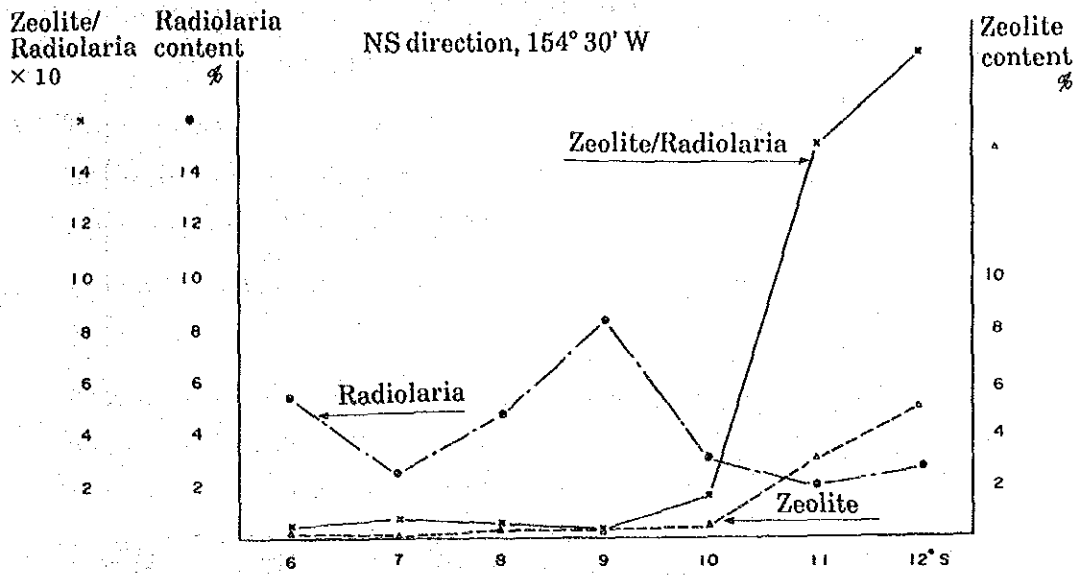


Figure 3-3-1 Characteristics of Bottom Materials (1)

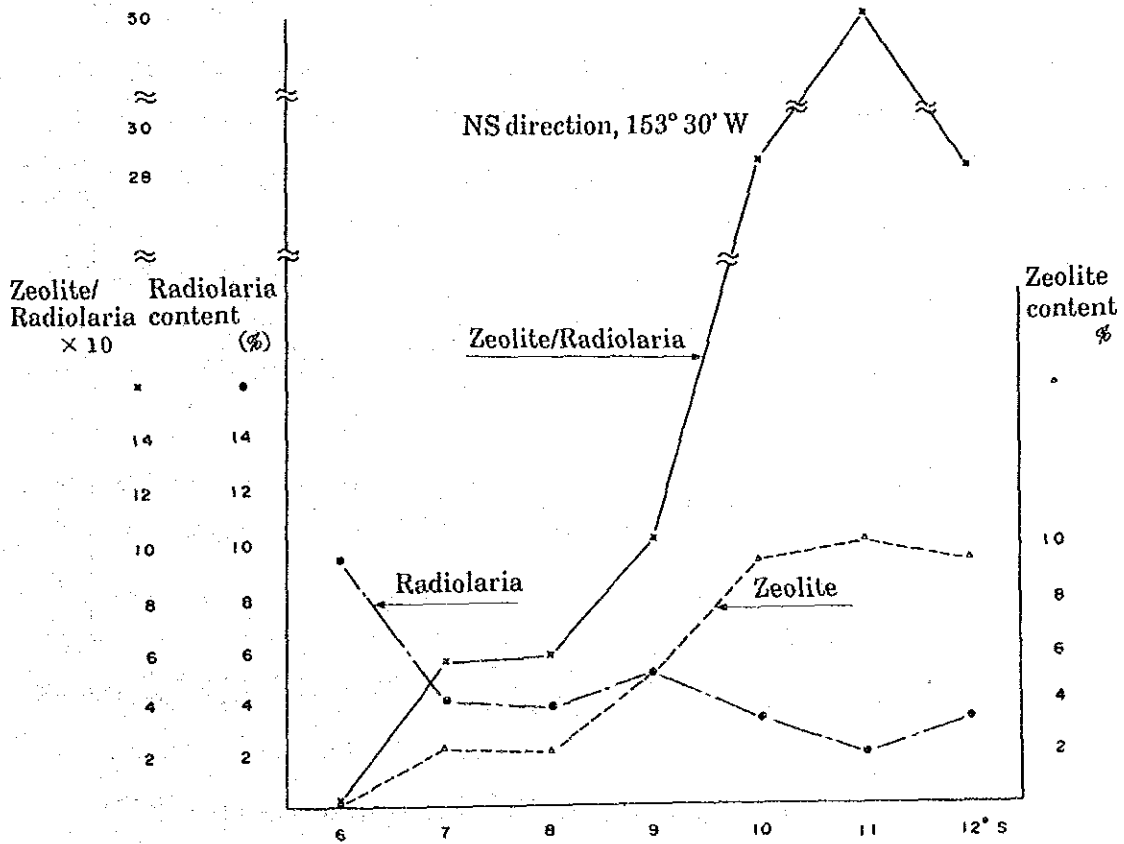


Figure 3-3-2 Characteristics of Bottom Materials (2)

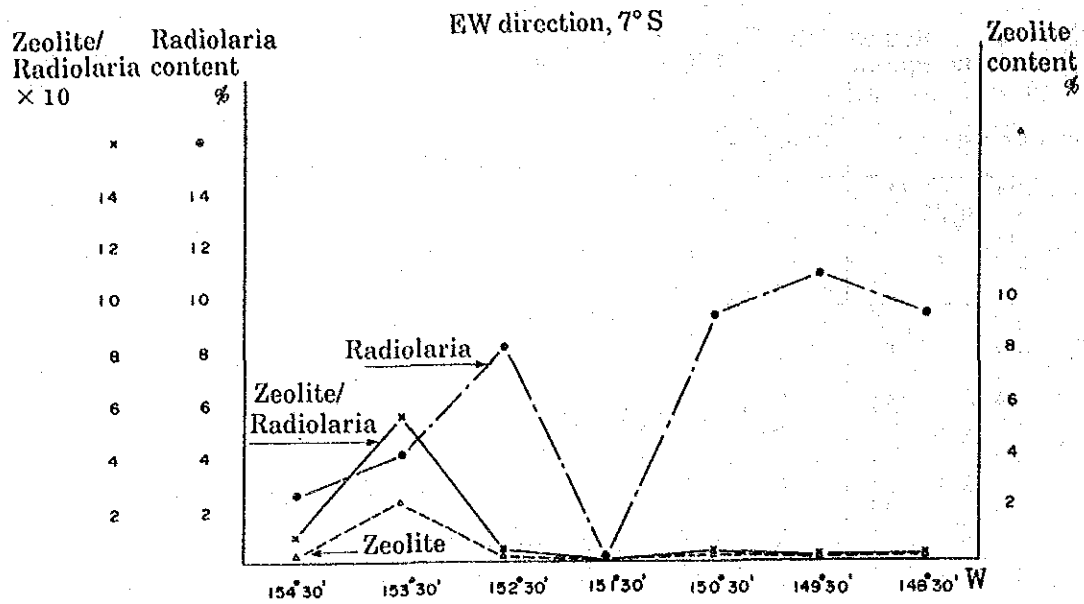


Figure 3-3-3 Characteristics of Bottom Materials (3)

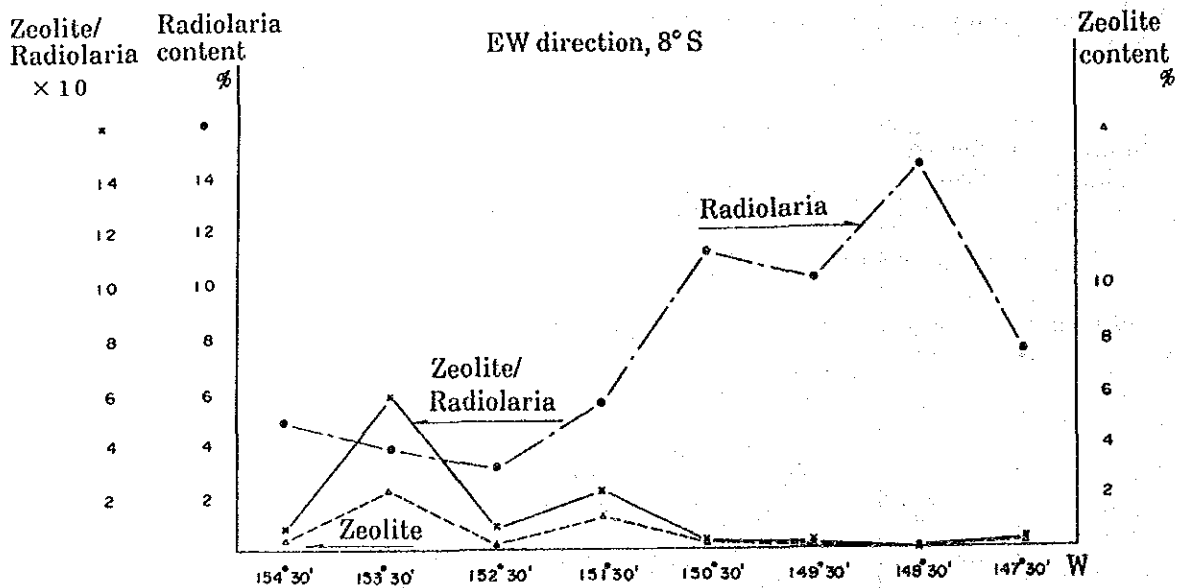


Figure 3-3-4 Characteristics of Bottom Materials (4)

In the NS direction, predominant at 9°S, and in the EW direction, predominant to the east of 150°30'W.

- ④ Fluctuation of zeolite content is observed. (Figure 3-3-1 to Figure 3-3-4).
In the NW direction, predominant to the south of 10°S and in the EW direction predominant in the west sea area.
- ⑤ ③ and ④ show that sea areas with high content of Radiolaria have low content of zeolite.
- ⑥ Among five SC, three have vertical observations of bottom materials with maximum length of 48cm and in the range of this length all of the species, size, color, texture etc., are identical.
- ⑦ Authigenic minerals (zeolite, clay minerals etc.) are observed among the samples collected by FG and SC except in the southern part of the west sea area (deeper than 5,200m).

4) Mineral Composition

X-ray powder diffraction of bottom materials collected by spade corer was carried out for mineralogical investigation and also for the observation of horizontal and vertical variation of the mineral composition.

Samples are collected by spade corer at two points in the northern sea (western sea area off the Line Islands: 89S0842SC01, and Eastern sea area off the Line Islands: 89S0846SC01) and one point in the southern sea (western sea area off the Line Islands: 89S1341SC01).

X-ray powder diffraction was carried out on every sample by bulk and oriented samples and, if necessary, hydrochloric acid treatment and ethylene glycol treatment were carried out as well.

The results of X-ray diffraction are shown in Table 3-3-3.

Typical chart is shown in Figure 3-3-5. Characteristics of bottom materials in the survey area are as follows;

- ① Mainly composed of clay minerals such as montmorillonite and illite accompanied by quartz and plagioclase.
- ② All the test pieces have small or medium amounts of phillipsite. This fact is also identified by microscopic observation.

- ③ The test pieces from the southwestern tip of the sea area (89S1341SC01) have only small amounts of illite content but contain more plagioclase than other test pieces. On the contrary, the test pieces collected at the northern part of the sea area (89S0842SC01, 89S0846SC01) have small and medium amounts of illite but very little plagioclase. These results show the existence of regional differences.
- ④ Differences according to the depth are not observed, but the samples collected at 89S0842SC01 show an increase of illite content at the depths below 40cm.

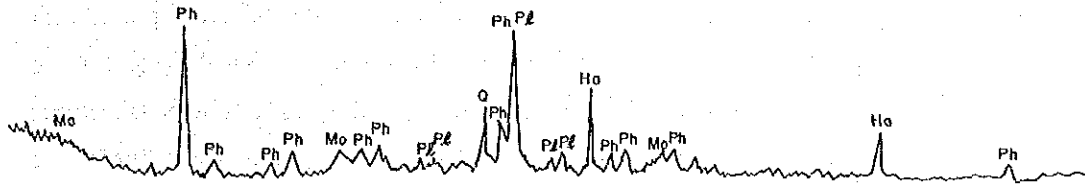
Table 3-3-3 Results of X-ray Diffraction Analysis of Bottom Materials

No.	Sample No.	Depth Surface	Silicate Minerals					*1 Halite
			Phillip-site	Montmorillonite	Illite	Quartz	Plagioclase	
1	89S1341SC01	Surface	○	△	×	×		△
2	89S1341SC01	10cm	○	△	×	×	×	△
3	89S1341SC01	20cm	○	△	×	×	×	△
4	89S1341SC01	30cm	○	△	×	×	×	△
5	89S1341SC01	40cm	○	△	×	×	×	△
6	89S0842SC01	Surface	○	×	△	×		○
7	89S0842SC01	10cm	○	△	△	×	×	△
8	89S0842SC01	20cm	○	△	△	×		△
9	89S0842SC01	30cm	○	△	△	×		△
10	89S0842SC01	40cm	○	△	○	×		△
11	89S0842SC01	48cm	○	×	○	×		△
12	89S0846SC01	Surface	△	△	△	×	×	○
13	89S0846SC01	10cm	△	△	△			△
14	89S0846SC01	20cm	△	△	△			△
15	89S0846SC01	30cm	○	△	×	×	△	△

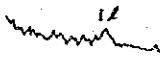
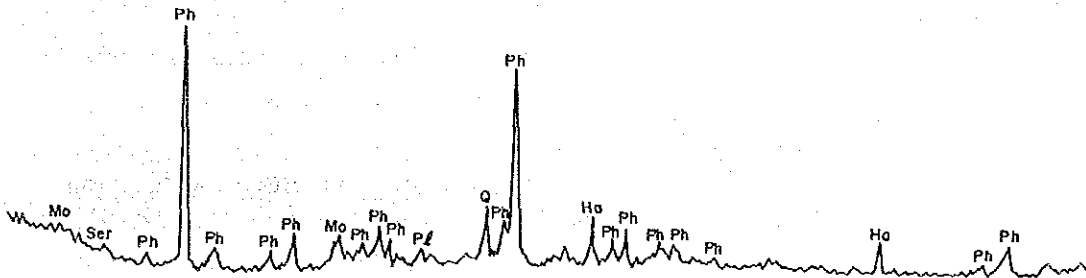
Legend ◎: Abundant ○: Common △: Little ×: Very little

*1 Halite is presumed to be the precipitated material from sea water contained in samples.

No.1 89S1341 SCOI Surface Bulk

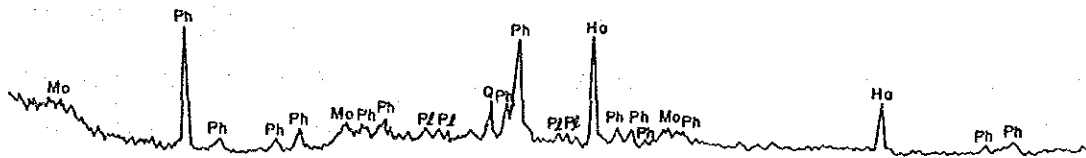


No.5 89S1341 SCOI 40cm Bulk



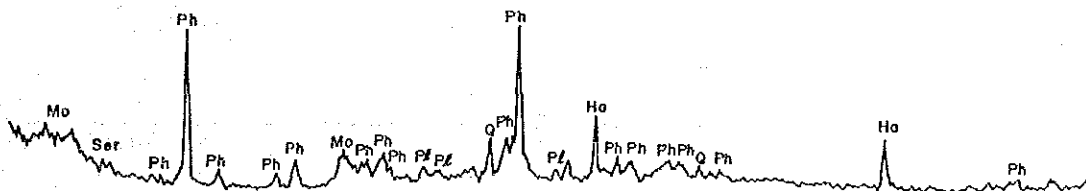
HCl treatment

No.6 89S0842 SCOI Surface Bulk



EG treatment

No.7 89S0842 SCOI 10cm Bulk

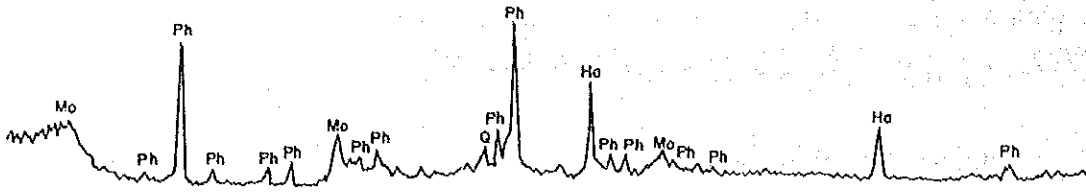


4° 10° 20° 30° 40° 50° 55°
(2θ)

Legend Q: Quartz Pl: Plagioclase Mo: Montmorillonite Il: Illite
Ser: Sericite Ph: Phillipsite Ha: Halite

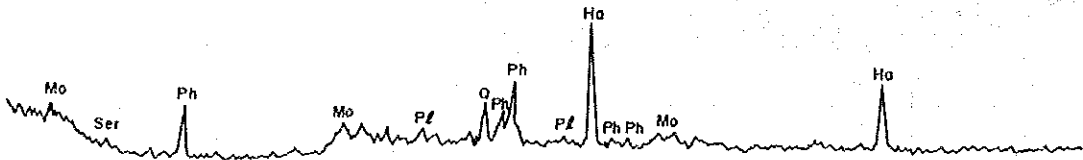
Figure 3-3-5 Typical X-ray Diffraction Patterns of Bottom Materials (1)

No.11 89S0842 SC01 48cm Bulk

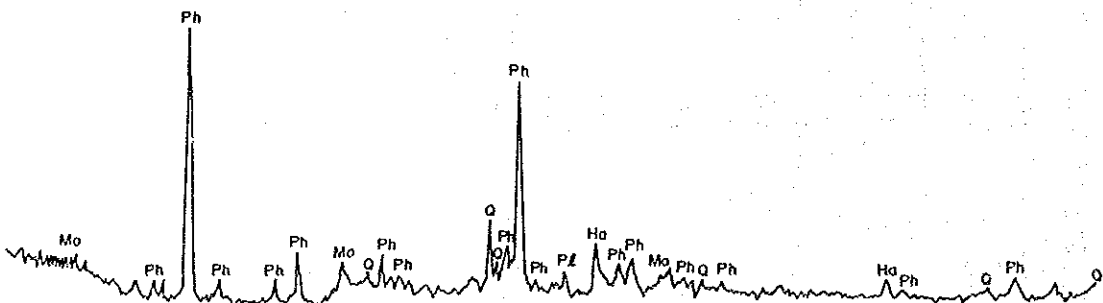


EG treatment

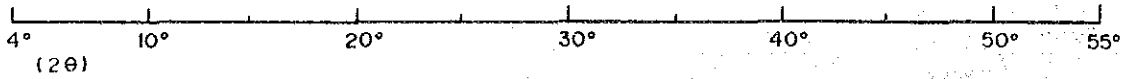
No.12 89S0846 SC01 Surface Bulk



No.15 89S0846 SC01 30 cm Bulk



HCl treatment



Legend Q : Quartz Pl : Plagioclase Mo : Montmorillonite Il : Illite
 Ser : Sericite Ph : Phillipsite Ha : Halite

Figure 3-3-5 Typical X-ray Diffraction Patterns of Bottom Materials (2)

5) Chemical Composition

The test pieces of spade core collected at same points as the test pieces subjected to X-ray diffraction were classified according to depth and were examined by chemical analysis of principal components and minor components. Results of the chemical analysis are shown in Table 3-3-4.

The characteristics of the bottom materials of this area are as follows:

- ① Compared with the chemical composition of DOMES sample, SiO_2 content is lower and Fe_2O_3 , MnO are higher in the present area. The dark reddish brown color of the bottom materials, as previously stated in section 2) is presumably caused by these content. It is inferable that both Fe_2O_3 and MnO are the effect of micro manganese nodules contained in the bottom materials.
- ② Na_2O content is high in the components of CaO , Na_2O and K_2O ; this might be caused by Na-rich phillipsite.
- ③ None of the minor components are worthy of special mention. However, as for Ni, Cu and Co the principal metals of manganese nodules, Cu content is higher than the others in all except sample No. 15.

6) Appraisal of Fossils

Identification of fossils was undertaken on Radiolaria and Foraminifera, taken from the bottom materials collected by the spade corer, to study the age and sedimentary environment of the bottom materials.

The test pieces were collected by spade corer at three sampling points and collected at intervals of 10cm in the following manner;

89S0842SC01 : surface layer, 10cm, 20cm, 40cm, 48cm.

89S0846SC01 : surface layer, 10cm, 20cm, 30cm.

89S1341SC01 : surface layer, 10cm, 20cm, 30cm, 40cm

(1) Radiolaria

① Method of analysis

About 10cc of test material was removed by inserting two pipes with diameters of 20mm into the vertical split section of the core. Every test piece was washed with water and the Radiolaria was enriched by sieve with the aperture of $62\mu\text{m}$, then cleaned with hydrochloric acid, hydrogen peroxide and hexametha-sodium phosphate, furthermore washed by water

Table 3-3-4 Chemical Composition of the Bottom Materials

(%)

No.	Sample	Components and Values													
		SiO ₂	TiO ₂	Al ₂ O ₃	Fe ₂ O ₃	FeO	MnO	MgO	CaO	BaO	Na ₂ O	K ₂ O	P ₂ O ₅	Ig-loss	
1	Surface	40.09	1.02	13.78	9.73	<0.01	2.49	3.26	3.50	0.07	7.70	3.14	1.19	12.11	
2	10 cm	42.45	1.08	14.32	9.94	<0.01	2.53	3.15	3.64	0.08	6.42	3.25	1.18	10.01	
3	20 cm	42.80	1.10	14.46	9.72	<0.01	2.50	3.08	3.72	0.07	6.36	3.41	1.22	9.58	
4	30 cm	43.55	1.10	14.36	9.75	<0.01	2.43	3.01	3.75	0.06	6.20	3.46	1.33	9.35	
5	40 cm	43.43	1.10	14.46	9.89	<0.01	2.42	2.97	3.59	0.08	6.01	3.53	1.36	9.50	
6	Surface	42.72	0.68	12.27	7.70	<0.01	2.12	3.34	4.06	0.12	7.50	2.73	1.63	13.08	
7	10 cm	43.58	0.76	13.35	8.56	<0.01	2.35	3.37	4.31	0.12	5.79	3.02	1.80	10.59	
8	20 cm	45.09	0.76	13.50	8.65	<0.01	2.22	3.34	4.32	0.10	5.44	3.19	1.68	9.86	
9	30 cm	44.62	0.75	13.27	8.55	<0.01	2.21	3.39	4.32	0.06	5.61	3.20	1.81	9.92	
10	40 cm	45.69	0.71	13.37	8.09	<0.01	2.17	3.62	4.36	0.10	5.46	3.14	1.86	9.61	
11	48 cm	45.94	0.57	13.06	7.27	<0.01	2.27	4.03	4.26	0.12	5.68	2.92	1.79	9.81	
12	Surface	44.41	0.66	11.48	7.95	<0.01	2.18	3.45	3.88	0.21	6.89	2.43	1.43	13.18	
13	10 cm	46.12	0.69	11.68	8.34	<0.01	2.18	3.50	3.78	0.22	6.52	2.35	1.27	12.36	
14	20 cm	44.28	0.71	12.68	8.72	<0.01	2.27	3.66	4.15	0.25	5.99	2.76	1.44	10.94	
15	30 cm	45.98	0.45	12.91	7.00	<0.01	2.13	2.74	4.97	0.31	5.21	4.29	2.14	9.18	
	X	51.5	0.59	12.5	5.4	—	0.53	1.5	3.0	1.5	—	5.7	3.3	11.2	

-14-

No.	Sample	Components and Values													
		Pb	V	B	Zn	Y	Ni	Cu	Co	As	Sr	Mo	Total		
1	Surface	0.008	0.023	0.016	0.014	0.027	0.035	0.042	0.027	0.004	0.036	0.011	98.33		
2	10 cm	0.008	0.023	0.016	0.015	0.030	0.035	0.042	0.026	0.004	0.037	0.012	98.31		
3	20 cm	0.008	0.023	0.016	0.014	0.031	0.036	0.043	0.026	0.003	0.038	0.014	98.28		
4	30 cm	0.008	0.020	0.016	0.015	0.032	0.036	0.043	0.026	0.003	0.036	0.014	98.61		
5	40 cm	0.008	0.020	0.016	0.031	0.032	0.036	0.044	0.025	0.004	0.034	0.016	98.62		
6	Surface	0.008	0.015	0.015	0.016	0.044	0.045	0.056	0.024	0.002	0.034	0.007	98.21		
7	10 cm	0.006	0.016	0.016	0.016	0.049	0.050	0.060	0.026	0.002	0.034	0.010	97.90		
8	20 cm	0.006	0.018	0.015	0.017	0.050	0.048	0.060	0.025	0.002	0.034	0.015	98.45		
9	30 cm	0.006	0.014	0.015	0.017	0.050	0.048	0.060	0.025	0.002	0.032	0.015	98.00		
10	40 cm	0.006	0.014	0.015	0.025	0.051	0.052	0.065	0.025	0.002	0.031	0.013	98.49		
11	48 cm	0.006	0.014	0.014	0.021	0.047	0.053	0.066	0.026	0.002	0.029	0.013	98.02		
12	Surface	0.005	0.017	0.016	0.020	0.036	0.045	0.056	0.022	0.002	0.034	0.011	98.42		
13	10 cm	0.005	0.012	0.016	0.015	0.035	0.041	0.051	0.021	0.002	0.034	0.011	99.26		
14	20 cm	0.005	0.012	0.014	0.022	0.040	0.047	0.057	0.023	0.002	0.036	0.015	98.13		
15	30 cm	0.005	0.012	0.015	0.016	0.043	0.049	0.037	0.022	0.001	0.035	0.018	97.57		
	X	—	—	0.17	—	—	—	—	—	—	—	—	—		

(%)

No. 1~15: Results of this Survey
X : DOMES Site - β (Bischoff J. L. et. al., 1979)

using the sieve with the same aperture of 62 μ m. After drying, the aforesaid specimen was sealed on the slideglass. Observation and identification were made by optical microscope to establish the list of principal radiolaria. Analysis of environment, age, etc., were carried out at the same time.

② Occurrence (Table 3-3-5, Figure 3-3-6)

[89S0842SC01]

Surface layer: An abundance of species and individuals, in a good state of preservation.

10cm : An abundance of species and individuals. State of preservation is not as good as that of the surface layer. Contains very small amount of unidentifiable Radiolaria that have already progressed to quartz.

20cm : An abundance of unidentifiable Radiolaria already progressed to quartz and of teeth of ichthyolite. Contains a small amount of identifiable Radiolaria.

30cm : An abundance of unidentifiable Radiolaria already progressed to quartz and of teeth of ichthyolite. Little identifiable Radiolaria.

40cm : An abundance of unidentifiable Radiolaria already progressed to quartz and of teeth of ichthyolite. No identifiable Radiolaria.

48cm : Extremely few unidentifiable Radiolaria already progressed to quartz. An abundance of teeth of ichthyolite.

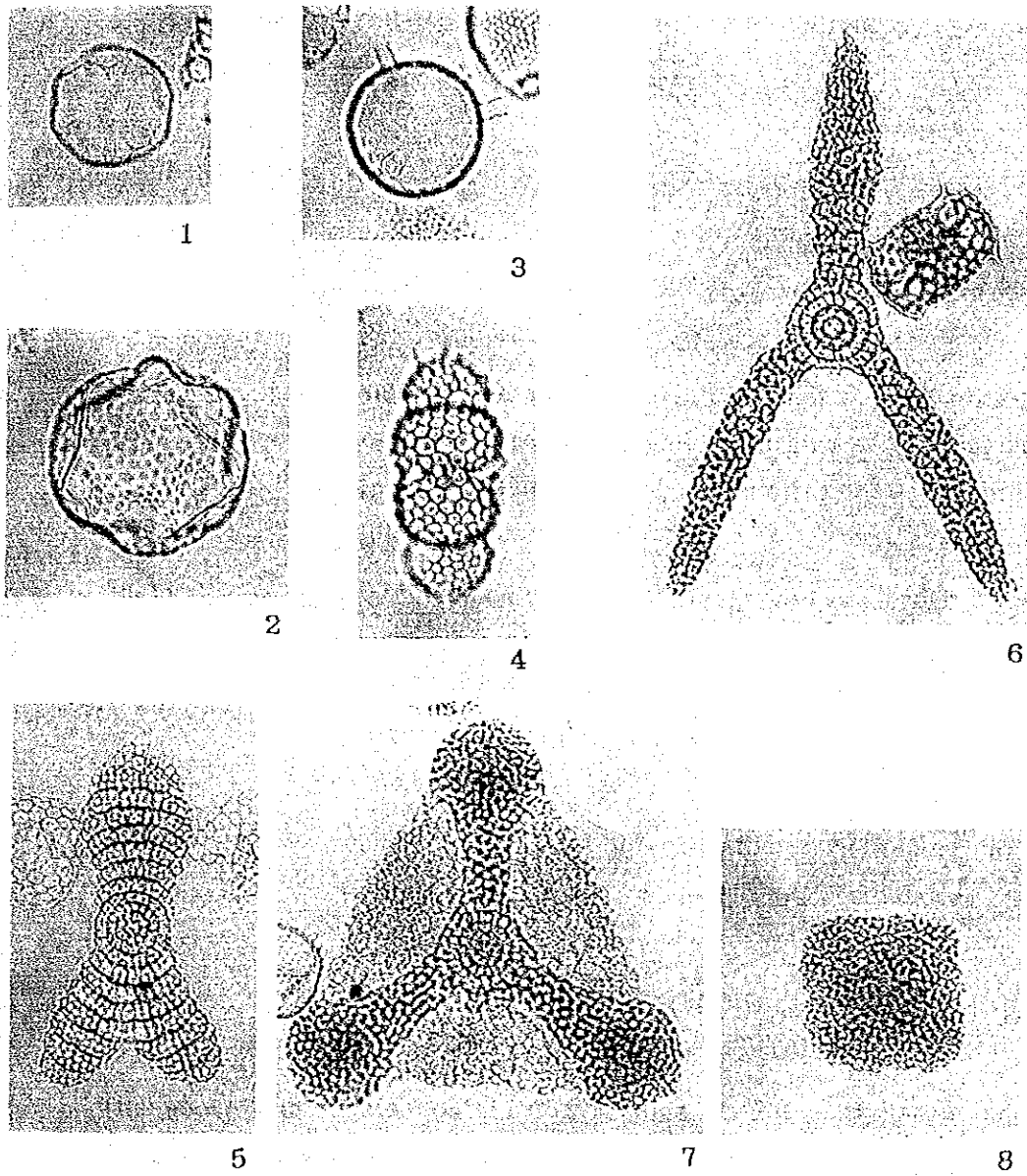
All of the Radiolaria identified from the test pieces collected between the surface layer and the 30cm layer are currently inhabitant species.

The upper two layers contain the species Buccinosphaera invaginata Haeckel which appeared about two hundred thousand years ago, also co-occurring with Collosphaera tuberosa Haeckel and Amphirhopalum ypsilon Haeckel which appeared about four hundred thousand years ago.

Radiolaria contained in the test pieces collected between the 20cm layer and 30cm layer are those of comparative abundance in the upper two layers

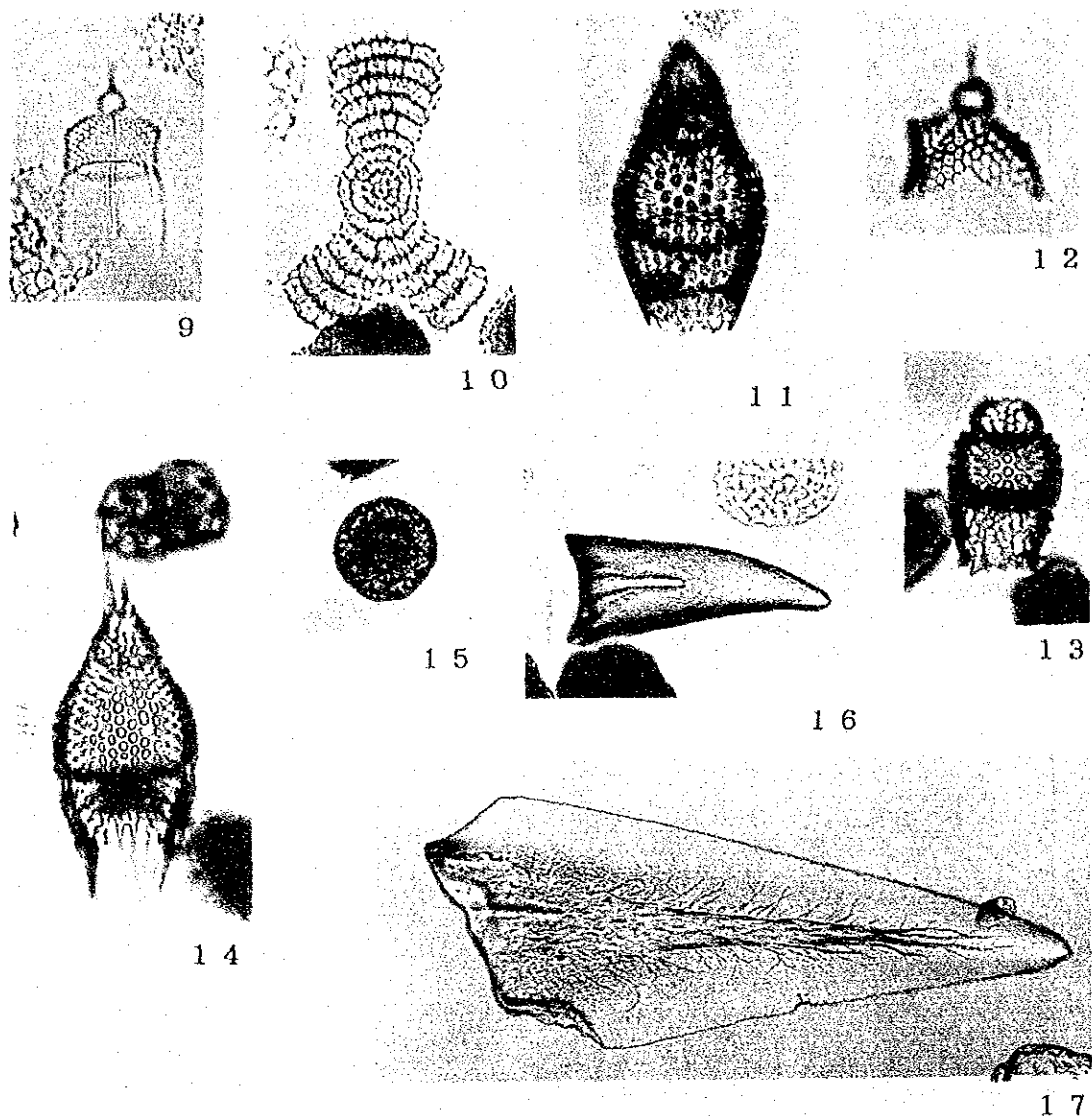
Table 3-3-5 List of Radiolarian Fossiles

Radiolarian Species	Samples					89S0042 SC01			89S0046 SC01			89S1341 SC01			
	1	10	20	30	40	48	1	10	20	30	1	10	20	30	40
Acrosphaera flammabunda (Haeckel)	X	X					X	X	X						X
A. lappacea (Haeckel)	X	X					X	X	X						
A. murrayana (Haeckel)	X	X					X	X	X						
A. spinosa Haeckel	X	X					X	X	X						
Buccinosphaera invaginata Haeckel	X	X					X	X							
Collosphaera huxleyi Muller	X	X					X	X							
C. tuberosa Haeckel	X	X					X	X	cf.						
Otosphaera polymorpha Haeckel	X	X					X	X	X						
Siphonosphaera socialis Haeckel	X	X					X	X	X						
Acanthosphaera capillaris Haeckel	X	X					X	X							
Actinomma medianum Nigrini	X	X					X	X							
A. spp.	X	X					X	X	X						
Actinosphaera capillacea (Haeckel)	X	X					X	X							
Amphisphaera cf. palliatum (Haeckel)	X	X					X	X							
Drupatruetus spp.	X	X					X	X	X						
Hexacantium spp.	X	X					X	X	X						
Hexacantium sp.	X	X					X	X	X						
Stylatractus nepocome (Haeckel)	X	X					X	X	X						
S. cf. neptunus Haeckel	X	X					X	X							
Thecosphaera radianus Holland et Enjuaet	X	X	X				X	X							
Xiphatractus sp.	X	X					X	X	X						
Omalarthus tetrahalanus (Haeckel) s.s.	X	X	X				X	X	X						X
Melioidiscus asteriscus Haeckel	X	X					X	X	X						
Amphitropalum ypsilon Haeckel	X	X					X	X							
Eucitonia elegans Ehrenberg	X	X					X	X	X						
E. frucata Ehrenberg	X	X					X	X	X						
Dictyocoryne profunda Ehrenberg	X	X					X	X	X						X
D. truncata (Ehrenberg)	X	X					X	X	X						
Spongaster tetras tetras Ehrenberg	X	X					X	X	X						
Spongodiscus biconcavus Ehrenberg	X	X					X	X	X						
Stylodictia spp.	X	X					X	X	X						
Xiphospira spp.	X	X					X	X	X						
Larcospira quadrangula Haeckel	X	X	X				X	X	X						
Tetrapyle octacantha Muller	X	X					X	X	X						X
GROSPHAERIDAE (Fragments)	X	X	X	X			X	X	X	X					X
Clathromitra pentacantha Haeckel	X	X					X	X							
Clathrocanium reginae Haeckel	X	X					X	X							
Pseudodictyophium glacialipes (Bailey)	X	X					X	X							
Botryocytis scutum (Harting)	X	X					X	X	X						
Carpocanium spp.	X	X					X	X	X						
Euceryphalus elizabethae (Haeckel)	X	X					X	X							
Eucyrtidium acuminatum Ehrenberg	X	X					X	X							X
E. anomalum (Haeckel)	X	X					X	X							X
E. dictyopodium (Haeckel)	X	X					X	X							
Lipmanella boobis (Haeckel)	X	X					X	X							
L. virchowii (Haeckel)	X	X					X	X							
Dictyophium infabricatum Nigrini	X	X					X	X							
Pterocanium charibdeum (Muller)	X	X					X	X	X						
P. praetextum (Ehrenberg)	X	X					X	X	X						
P. trilobium (Haeckel)	X	X					X	X							
Anthocyrtilidium ophirensis (Ehrenberg)	X	X					X	X	X						
A. zanguebaricum (Ehrenberg)	X	X					X	X							
Lamprocyclas maritima Haeckel	X	X			X		X	X	X						
Lamprocyrtilis gamphonycha (Jorgensen)	X	X					X	X	X						
Pterocorys hertwigii (Haeckel)	X	X					X	X							
P. macroceras (Popofsky)	X	X					X	X							
P. zancleus (Muller)	X	X					X	X							
Theocorythium trachelium (Ehrenberg)	X	X					X	X	X						
Botryostrobos aquilonaris (Bailey)	X	X					X	X	X						
B. auritus (Ehrenberg)	X	X					X	X	X						
Phrmostichoartus corbula (Harting)	X	X					X	X	X						
Spirocyrtilis scalaris Haeckel	X	X					X	X							
S. subscalaris Nigrini	X	X					X	X							
Tholospyris ramosa Haeckel	X	X					X	X							
T. acuminata (Hertwig)	X	X					X	X							
Acanthodesmia vuniculata (Muller)	X	X	X	X			X	X	X						X
Liriospyris reticulata (Ehrenberg)	X	X					X	X							
Nephtrosyris renilla Haeckel	X	X					X	X							
Amphitropalum praeypsilon Sakai									X						
cf. Eucyrtidium matuyamai Hays									X						
Pterocanium prismatium Riedel									X						
Sticochorys peregrina (Riedel)								X	X	X					
S. delmontensis (Campbell et Clark)									X						
Podocyrtilis papalis Ehrenberg									X						
Silicified Radiolaria	X	X	X	X	X	X	X	X	X	X	X	X	X	X	X



1. *Buccinosphaera invaginata* (89S0846SC01, 1cm)
2. *Collosphaera tuberosa* (89S0846SC01, 1cm)
3. *Siphonospaera socialis* (89S0842SC01, 1cm)
4. *Ommatartus tetralthalamus* (89S0846SC01, 1cm)
5. *Amphirhoparum ypsilon* (89S0846SC01, 1cm)
6. *Eucitonia elegans* (89S0846SC01, 1cm)
7. *Dictyocoryne profunda* (89S0846SC01, 1cm)
8. *Spongaster tetras* (89S0846SC01, 10cm)

Figure 3-3-6 Species of the Typical Radiolarian Fossils (1)



9. *Pterocanium praetextum* (89S0842SC01, 10cm)
10. *Amphirhoparum praeepsilon* (89S0846SC01, 20cm)
11. cf. *Eucyrtidium matuyamai* (89S0846SC01, 20cm)
12. *Pterocanium prismatium* (89S0846SC01, 20cm)
13. *Sticochorys delmontensis* (89S0846SC01, 20cm)
14. *Podocyrtis papalis* (89S0846SC01, 20cm)
15. Silicified Radiolaria (89S0846SC01, 30cm)
16. Ichthyolith (89S0846SC01, 20cm)
17. Ichthyolith (89S0846SC01, 30cm)

Figure 3-3-6 Species of the Typical Radiolarian Fossils (2)

and very few in quantity, they are assumed to be individuals mingled from upper layers.

[89S0846SC01]

Surface layer: An abundance of species and individuals, in a good state of preservation. Containing very few fragments of intensely etched Radiolaria-quartz.

10cm : Many species and individuals but not so well preserved as those of the surface layer. Contains a few fragments of intensely etched Radiolaria skelton and unidentifiable Radiolaria-quartz.

20cm : An abundance of comparatively well preserved Radiolaria, almost the same as those contained in the test pieces of the 10cm layer, as well as unidentifiable Radiolaria-quartz and teeth of ichthyolite. Also a few intensely etched Radiolaria.

30cm : An abundance of unidentifiable Radiolaria-quartz and teeth of ichthyolite. No identifiable Radiolaria.

All of the Radiolaria identified from the test pieces collected between the surface layer and 20cm layer are currently inhabitant species.

The upper two layers contain the species of Buccionsphaera invaginata Haeckel which appeared about two hundred thousand years ago and also co-occurred with Collosphaera tuberosa Haeckel and Amphirhopalum ypsilon Haeckel which appeared about four hundred thousand years ago. The community of etched Radiolaria of 20cm test pieces is composed of various species from the Eocene (Podocyrtris papalis Ehrenberg, etc.,) to the Pliocene (Pterocanium prismatium Riedel, etc.,).

[89S1341SC01]

Surface layer: Contains a few comparatively well preserved Radiolaria, an abundance of unidentifiable Radiolaria-quartz and teeth of ichthyolite.

- 10cm : A few unidentifiable Radiolaria-quartz. An abundance of teeth of ichthyolite. No identifiable Radiolaria.
- 20cm : Very few of unidentifiable Radiolaria-quartz. An abundance of teeth of ichthyolite. No identifiable Radiolaria.
- 30cm : Very few unidentifiable Radiolaria-quartz. An abundance of teeth of ichthyolite. No identifiable Radiolaria.
- 40cm : Very few unidentifiable Radiolaria-quartz. An abundance of teeth of ichthyolite. No identifiable Radiolaria.

All of the Radiolaria contained in the test pieces are currently inhabitant species. Compared with ordinary surficial sediments, the occurrence of Radiolaria is remarkably few. Also, in comparison with the zones where sediments are quite few, the state of preservation is extremely good.

③ Age and Sedimentary Environment

[89S0842SC01]

The test pieces of the surface layer and the 10cm layer contain the Collosphaera tuberosa Haeckel and the Amphirhopalum ypsilon Haeckel, which appeared at the latter period of the Quarternary, about four hundred thousand years ago, as well as the Buccinosphaera invaginate Haeckel which appeared about two hundred thousand years ago. Accordingly, the age of the upper parts of the 10cm layer is later than the last period of the Pleistocene of the Quarternary (less than two hundred thousand years old).

As the occurrences between the 10cm layer and the 20cm layer show a sudden change, an existence of unconformity during this period is estimated.

From the state of occurrence of the Radiolaria, currently inhabitant species, taken from the 20cm layer test piece, it is presumable that the Radiolaria of the upper layers intermingled into this layer. As no other effective Radiolaria are identified, age of the layers below this cannot be decided.

[89S0846SC01]

The test pieces of the surface layer and the 10cm layer contain the Collosphaera tuberosa Haeckel and the Amphirhopalum ypsilon Haeckel, which appeared at the latter period of the Quarternary, about four hundred thousand years ago, as well as the Buccinosphaera invaginata Haeckel, which appeared about two hundred thousand years ago. The age of the sediments above the 10cm layer is later than the last period of the Pleistocene of the Quarternary (about two hundred thousand years).

The Radiolaria contained in the test piece of the 20cm layer is mainly composed of the species of the Pleistocene period, and those of the Eocene to the Pliocene periods. Below this layer (30cm) sediments accompanied by Radiolaria-quartz, the age of which is unidentifiable, are observed. An inference is made that the zone was under the non-sedimentary or exfoliating environment from the latter period to the last period of the Pleistocene, and that the unconformity was formed between the 20cm layer to the 30cm layer.

After that (about two hundred to three hundred thousand years ago), this place became a sedimentary site for Radiolaria remains and, at an early stage, Radiolaria of the Eocene and Pliocene were washed out from the peripheral sediments into this zone.

[89S1341SC01]

It is impossible to decide the age and the rate of sedimentation.

④ Sedimentation Rate

[89S0842SC01]

If, as previously stated, the age of the 10cm layer was later than two hundred thousand years, the average sedimentation rate would be more than 0.5mm/1,000 year. It is impossible to estimate the sedimentation rate for the layers below 20cm due to the lack of data for determining the time factor.

[89S0846SC01]

If, as previously stated, the age of the 10cm layer was later than two hundred thousand years, the average sedimentation rate would be more than 0.5mm/1,000 year. It is impossible to estimate the sedimentation rate of the layers below 20cm.

[89S1341SC01]

It is impossible to estimate the sedimentation rate because of no data is available. There is no established theory on what environmental conditions caused the dissolution of Radiolaria, but obvious dissolution is observed in the zones with a sedimentation rate of below 1mm/1,000 years. Almost all of the Radiolaria at the zones with the sedimentation rate of under 0.1mm/1,000 years were dissolved entirely. No remarkable dissolution is observed on the Radiolaria of the Pleistocene period in the layers above 10cm of [89S0842SC01] and [89S0846SC01], so it is assumed that the sedimentation rate of neighboring layers must be around 1mm/1,000 years.

⑤ Paleo-environment and others

[89S1341SC01]

The Radiolaria (currently inhabitant species) contained in the test piece of the surface layer of [89S1341SC01] are very few in number compared with the normal surficial sediments, and the state of preservation is extremely good compared with that of zones with very few sediments. The species of Radiolaria identified here are the same as normally seen in the low latitude Pacific Ocean. From this fact, the state of preservation of the said test piece is to be considered as same as that of the 20cm-layer of [89S0842SC01]. The remains composed of currently inhabitant Radiolaria accumulated on the upper layer of unfossilized sediments at the sedimentation rate of more than 1mm/1,000 years. And then, by some kind of chaos, a part of them intermingled into the layers of the test piece, which was in the state of non-fossilization. As the test piece was located on the uppermost part of the core, it is conceivable that there had been some sediments, which contained a large amount of Radiolaria in good state of preservation, on the test piece layer. This sediment might have

been out or exfoliated.

[89S0846SC01]

Among the etched Radiolaria population contained in the test piece of the 20cm layer, there are specimens different ages such as the Eocene (Podocyrthis papalis Ehrenberg, etc.), the Miocene (Stichocorys delmontensis (Chambell et Clark), etc.) and the Pliocene (Pterocanium prismatium Riedel, etc.). From those different aged sediments, different species of Radiolaria were washed out and re-accumulated on the surface of an unconformity. At that time there must have been places around there where the sediments of those ages were exposed on the sea floor. Therefore, if data of location, layers of exfoliation, relative height, etc., are available, it might be possible to study the process of formation and extent of the interface of unconformity. Furthermore, even if the sediments of aforesaid ages are existing in the vicinity, they must be covered by sediments accumulated later than the last period of the Pleistocene from the fact that there are scarcely any of the re-accumulated Radiolaria in the uppermost portion of the core.

(2) Foraminifera

① Method of analysis

About 30gr. of the wet test piece was mudded by adding warm water and laid out for a whole day, then washed on a 200-mesh (0.074mm) seive and dried. The grains of residuum were scattered carefully so as not to overlap each other on a measured chalet and then every individual of the Planktonic and Benthic Foraminifera Fossil was picked out and identified under the stereomicroscope.

② Occurrence (Table 3-3-6, Figure 3-3-7)

No Planktonic Foraminifera Fossils are found in the test pieces.

Benthic Foraminifera Fossil Population

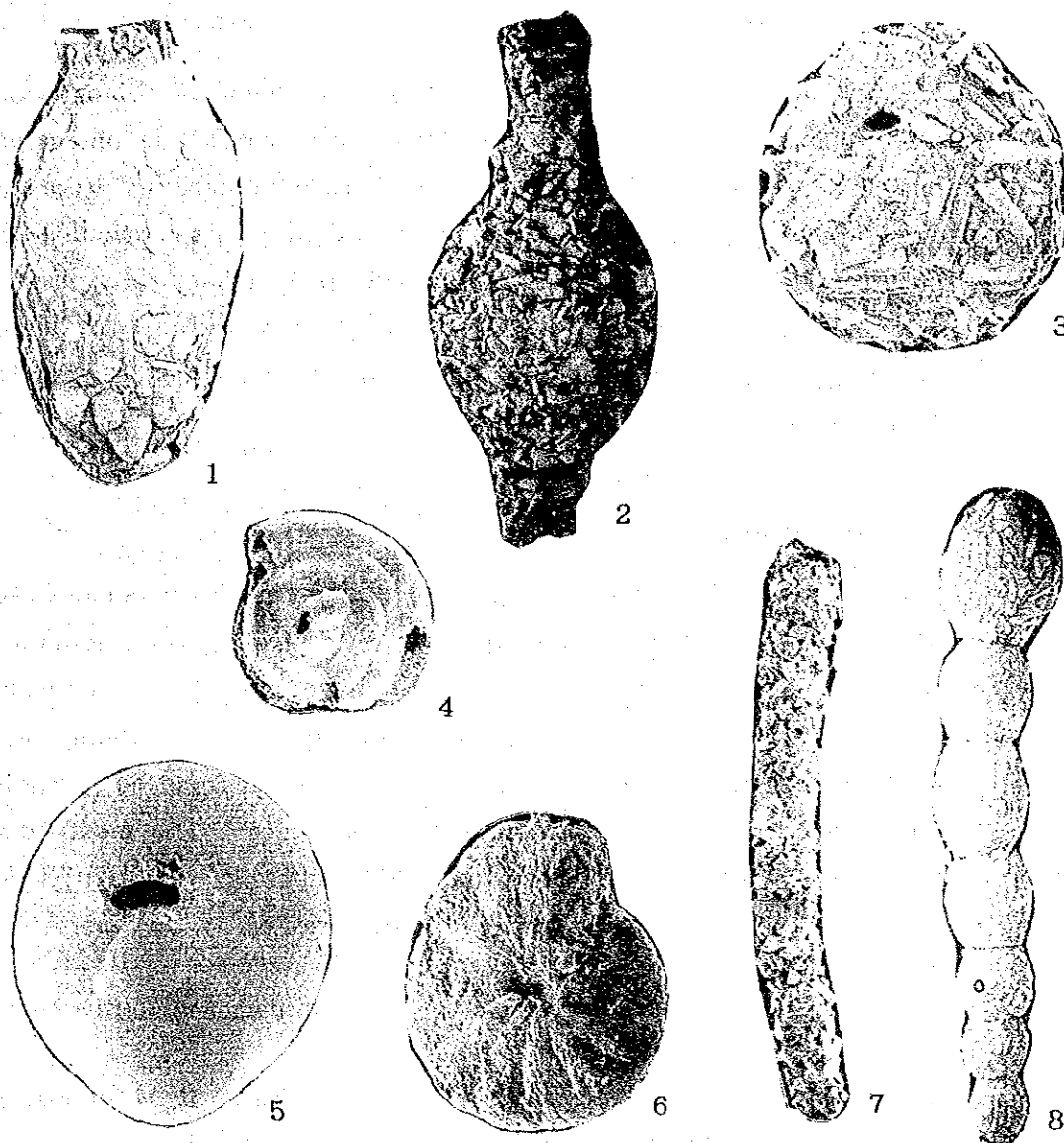
[89S0842SC01]

The test pieces from the surface layer to the 48cm depth are homogeneous red clay when observed by the unaided-eye. The treated test pieces

contain micro nodules and teeth of ichthyolite. No occurrence of nodules with as large as those of the 10cm-layer of the [89S1341SC01] is observed from these test pieces. A large amount of Benthic Foraminifera Fossil Populations occur in the surface layer but in the layers deeper than 10cm, the number of individuals drops abruptly. A population mainly composed of psamitic shell Bathysiphon sp. accompanied with psamitic shell Benthic Foraminifera Fossils such as Haplophragmoides sp., Reophax sp., etc., are observed. Continuous occurrence of Bathysiphon sp. is observed below 10cm though the quantity is few. Reophax distans is the most prominent Benthic Foraminifera population at the depth of 30cm.

Table 3-3-6 List of Foraminifera Fossils

Species	Samples	89S0842SC01					89S0846SC01				89S1341SC01					
		Surface	10 cm	20 cm	30 cm	40 cm	48 cm	Surface	10 cm	20 cm	30 cm	Surface	10 cm	20 cm	30 cm	40 cm
Agglutinated Foraminifera																
Alveophragimium sp. (frag.)			1	2				1					1			
Ammobaculites sp.												1				
Ammodiscus sp.	1															
Ammoscalaria ? sp.				1												
Bathysiphon sp.	23	2	1		1	1	3		3	3	4	2				2
Cyclammina cf. compressa	1											1				
Cyclammina pusilla							1									
Cyclammina sp.						1										
Cystammina galeata	1															
Cystammina sp.											1					
Haplophragmides sp.	3	1														
Reophax nodulosus	1															
Reophax distans				6												
Reophax sp.	2				1											
Saccammina sp.					1	1										
fragment (unknown)							1			3	2					
Total	32	4	3	7	3	3	5	1	3	6	8	4	0	0	0	2



Microscopic Photographs of Typical Species

1. *Reophax* sp. (89S0842SC01, Surface, ×100)
2. *Reophax distans* (89S0842SC01, 30cm, ×200)
3. *Haplophragmoides* sp. (89S0842SC01, Surface, ×100)
4. *Ammodiscus* sp. (89S0842SC01, Surface, ×200)
5. *Cystammina galeata* (89S0842SC01, Surface, ×150)
6. *Cyclammina* cf. *comprssa* (89S1341SC01, 10cm, ×150)
7. *Bathysiphon* sp. (89S0842SC01, Surface, ×150)
8. *Reophax nodulosus* (89S0842SC01, Surface, ×150)

Figure 3-3-7 Species of the Typical Foraminifera Fossils

[89S0846SC01]

The test pieces from the surface to the 30cm deep are homogeneous red clay when observed by the unaided-eye. The treated test pieces contain micro nodules and teeth of ichthyolite. Most of the nodules from the test pieces have a diameter of about 2mm, and large sized nodules such as occurred at the 10cm layer of [89S1341SC01] are not recognised. Very few individuals occur in the layers from the surface to 30cm and Bathysiphon sp. occurs continuously in the layers with the exception of 10cm layer.

[89S1341SC01]

The test pieces from the surface to 40cm deep are homogeneous red clay when observed by the unaided-eye. The treated test pieces contain micro nodules and teeth of ichthyolite. The maximum diameter of the nodules is about 15mm, which occurred in the 10cm layer. As a whole, very few Benthic Foraminifera observed from the test pieces and no Foraminifera Fossils are recognized from the 30cm test piece. The most numerous population in the surface, 10cm and 40cm layers is the Bathysiphon sp. (psamitic shelled). No Calcareous Foraminifera Fossils are observed.

③ Geologic Age

As no Planctonic Foraminifera Fossils occur here, it is impossible to estimate the Geologic Age from the Foraminifera Fossil.

④ Paleo-environment

[89S0842SC01]

Comparatively large amount of Benthic Foraminifera Fossils occur at the surface layer but the occurrence of Foraminifera Fossil drops abruptly below 10cm. The Reophax distans (psamitic shelled) is prominent at the 30cm layer of [8S0842SC01] while the Bathysiphon sp. occurs continuously in the surface, 10cm, 20cm, 40cm and 48cm layers with the exception of the 30cm layer. All of the species occurred belong to the psamitic shell species. The Paleo-environment below the CCD is estimable.

[89S0846SC01]

As a whole, very few Foraminifera Fossils and only a few Benthic Foraminifera Fossils (psamitic shelled) are recognized. Most of them are of Bathysiphon sp.

All of the species belong to the psamitic shell species and none of the calcareous shell species are found. The sedimentary environment below the CCD is estimable.

[89S1341SC01]

The Paleo-environment (sedimentary environment) of the 20cm and 30cm layers are not estimable due to the absence of Foraminifera Fossils. Most of the individuals occurring in the surface, 10cm and 40cm layers are presumed to be the population of the Bathysiphon sp. (psamitic shelled) and the sedimentary environment below the CCD is estimable.

7) CCD (Calcium Carbonate Compensation Depth)

If we consider the maximum water depth where the existence of calcium carbonate minerals terminates to be the Calcium Carbonate Compensation Depth, the observation of smear slides by microscope indicates that the CCD in the survey area will be around 5,000m.

3-4 MFES Survey of Manganese Nodules

1) Comparison with Sampling Results

The relation between estimated abundance of manganese nodules by MFES and sampling results for each sampling station is shown in Figure 3-4-1.

From the figures (a), (b) and (c) of the Figure 3-4-1, following features are indicated;

(1) Influence of topography

Correlation between MFES and sampling data is inconsistent in the case of seamounts and sea knolls. Such phenomena appear often, and it is considered that in areas of steep topography, side echo would be too strong for normal sound pressure.

Zones other than seamounts and sea knolls show consistent results of correlation between MFES and sampling data as shown in Figure (c), though the abundance is as low as 0~5 kg/m².

(2) Correlation with SBP Type

Comparison between figure (a) and figure (b) shows that sampling stations of seamounts and sea knolls indicate the acoustic opaque of the types ds, d₁ and d₂. In the sea area of Clarion-Clipperton zone, MFES showed false abnormality of these types, therefore, application of MFES was excluded. However, the sampling data shows this area has high abundance at the depth of the CCD, or high seamounts and sea knolls. Accordingly, it is desirable to pay attention to those seamounts situated above the level of the CCD with indications of type ds, type d₁ and type d₂, even if the values of MFES are low.

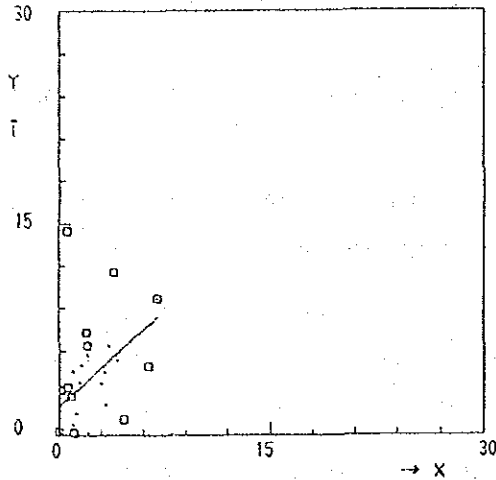
2) MFES Estimation of Manganese Nodule Abundance

Estimated Abundance Map of Manganese Nodule by MFES is shown in Annexed Figure 7. Comparatively high values of 5~10 kg/m² are recognized at the western and eastern parts of the sea area, but barren regions of 0~2 kg/m² are widely recognized. These barren regions are related to the prominence of type ds in the sea area, and the influence of the Line Islands line, which crosses the central part of the sea area in the NW-SE direction, is conceivable.

Distribution classified by topography is as follows :

- Plains** : High values of 5~10 kg/m² are recognized to the south of 8°S.
Barren regions of 0~2 kg/m² are recognized to the north of 8°S.
- Hills** : 4~10 kg/m² are recognized in the neighborhood of (7°S, 152°W), the rest are barren regions of 0~2 kg/m².
- Mountainous regions:** Indicating 0~2 kg/m², most of the seamounts show type ds and type d₁. Occurrence of manganese nodules is not expected but cobalt crusts are promising.
- Quasi-plains** : Indicating type d₂ around water depth of 4,800m, high values of 5~10 kg/m² are recognized. These features are consistent with the sampling results. Abundance of manganese nodules occurring by calcareous sediments around CCD depth is conceivable.

X axis: Amended MFES Value (kg/m²)
 Y axis: Sampling abundance (kg/m²)



- STATISTICS -

Coefficient = .50

(a) Classification by topography

$$A = .90$$

$$B = 2.03$$

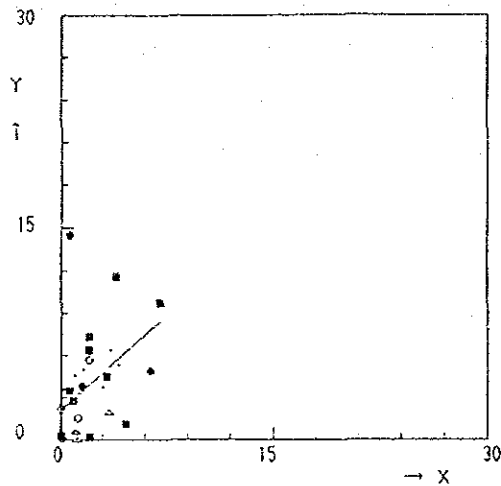
$$Y = A * X + B$$

$$N = 32$$

□ : Seamount, sea knoll

· : Fresh sediments

X axis: Amended MFES Value (kg/m²)
 Y axis: Sampling abundance (kg/m²)



- STATISTICS -

Coefficient = .50

(b) Classification by SBP type

$$A = .90$$

$$B = 2.03$$

$$Y = A * X + B$$

$$N = 32$$

SBP type

· : e₁

□ : t_s

■ : d_s

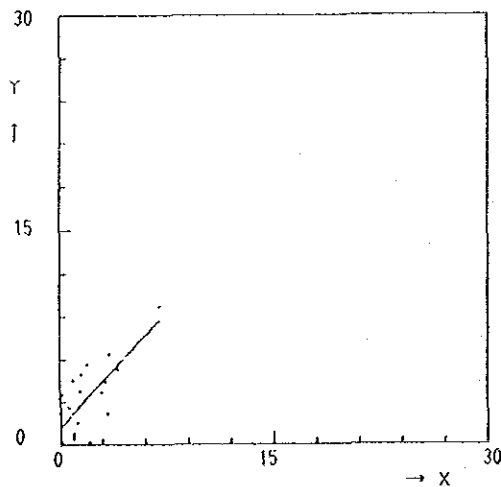
• : d₁ or d₂

○ : c

+ : a

△ : b

X axis: Amended MFES Value (kg/m²)
 Y axis: Sampling abundance (kg/m²)



- STATISTICS -

Coefficient = .74

(c) Exclusion of seamounts and sea knoll

$$A = 1.07$$

$$B = 1.22$$

$$Y = A * X + B$$

$$N = 19$$

□ : Seamount, sea knoll

· : Fresh sediments

Figure 3-4-1 Relation between MFES and Sampling Results

3-5 Modes of Manganese Nodule Occurrence

The modes of occurrence of manganese nodules were summed up as follows by analyzing the samples, results of observation and sea bottom photographs.

1) Morphology, Size Distribution and Occurrence

Morphology and size distribution were based on the same standard as that for past years.

(1) Morphology

Manganese nodules appeared in this area were classified into seven types as follows:

- ① Spheroidal type : Nearly perfect sphere.
- ② Ellipsoidal type : Divided into normal and fat types. Normal type has hamburger-shaped external form and crushed spheroidal form. Flat type is thicker than the normal type.
- ③ Pebble thin type : This type is like small pebbles on the sea shore or like a "go" stone with a relatively smooth surface without irregularly.
- ④ Pebble type : This type looks like gravel or pebbles on a shore or in a river bed, (with a diameter of approx. 2~4 cm).
- ⑤ Massive type : Irregular and angular shape (including various shapes such as spheroidal, ellipsoidal or thick plate).
- ⑥ Plate type : Thin and round in shape like roof shingles or rice cakes.
- ⑦ Others : Manganese nodules which cannot be classified into above six types.

Several photographs of typical shape of manganese nodules are shown in Figure 3-5-3. Distribution of manganese nodules is shown in Annexed Figure 8. The morphology and sampling weight of manganese nodules is shown in Figure 3-5-1.

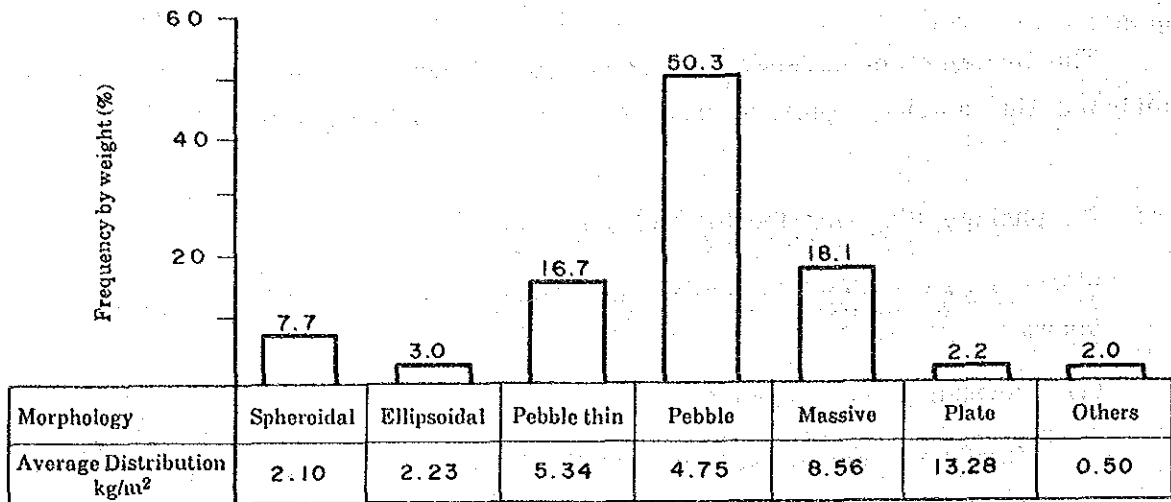


Figure 3-5-1 Morphology and Sampling Weight of Manganese Nodules

The following distinctive features were recognized:

- ① Rich in Pebble type (50.3%), Massive type (18.1%), Pebble thin type (16.7%), with very few of Ellipsoidal (3.0%).
- ② Pebble type was found everywhere, Spheroidal type had the tendency of emerging locally around higher points.
- ③ Frequency by weight for the Massive and Pebble thin types were different in the western and eastern seas off Line Islands, with more Massives in the western sea and more Pebble thin in the eastern sea.

	<u>Massive type</u>	<u>Pebble thin type</u>
Western Sea off Line Isl.	26.3%	5.3%
Eastern Sea off Line Isl.	11.1%	26.5%

(2) Size

Sampled manganese nodules were weighed according to size classification; they were classified by longitudinal diameters such as 0~2 cm, 2~4 cm, 4~6 cm, 6~8 cm, 8~16 cm. The result showed that the size of 2~4 cm is predominant in this sea area and its frequency by weight amounted to 49% of the whole sample. Other characteristics were as follows: (Fig. 3-5-2)

- ① Sizes of 0~2 cm and 2~4 cm amounted to 66%, this sea area is abundant in small sized manganese nodules.
- ② Size of 2~4 cm in the eastern sea off Line Islands amounted to 52%, and in the western sea 44%. Smaller sized manganese nodules occur widely in the eastern sea area.
- ③ Large sized (4~6 cm or more) nodules occur in the deep sea areas of the southern part of the western sea area.
- ④ Nodules with the size of 0~2 cm occur locally at higher elevations.

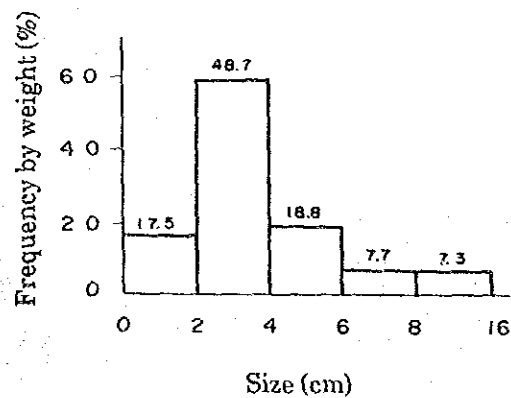


Figure 3-5-2 Size and Sampling Weight of Manganese Nodules

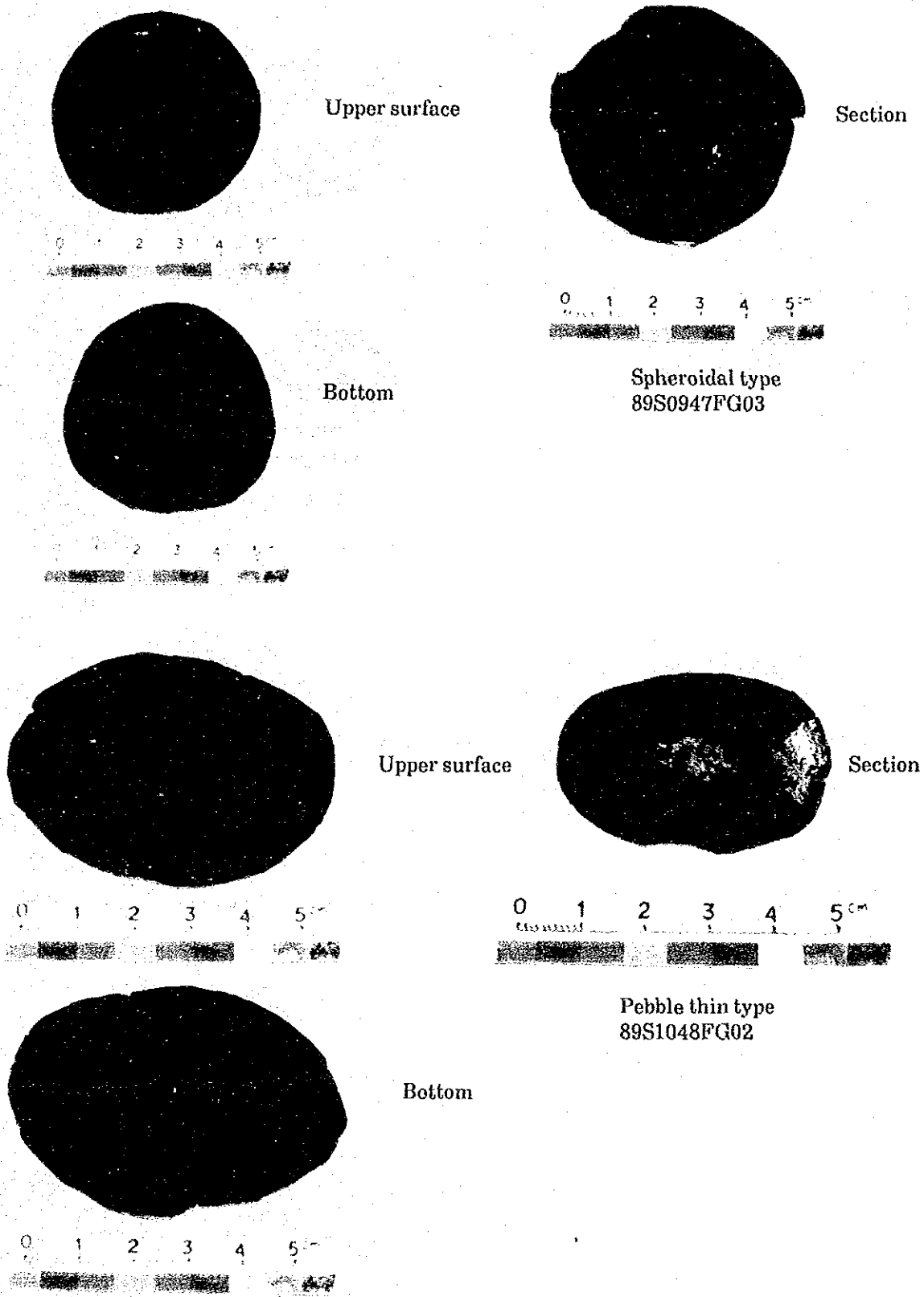
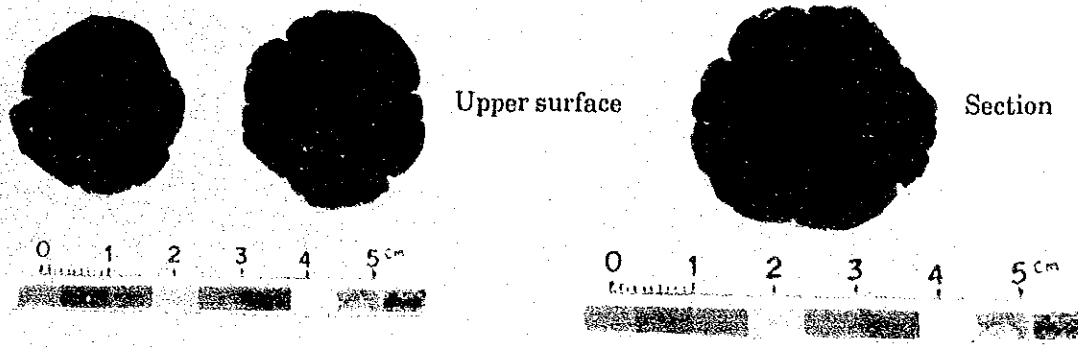
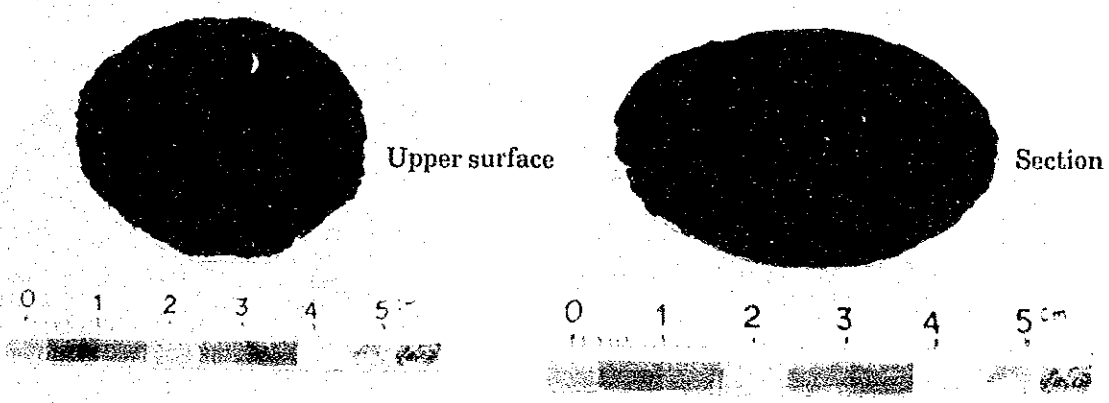
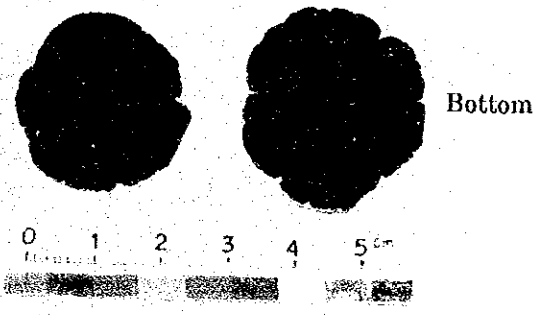


Figure 3-5-3 Morphology of Manganese Nodules (1)



Pebble type
89S0842FG02



Ellipsoidal type
89S0842SC01

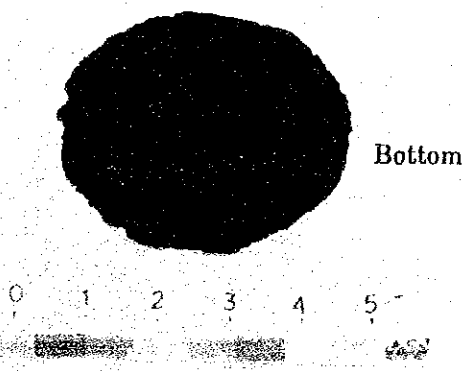
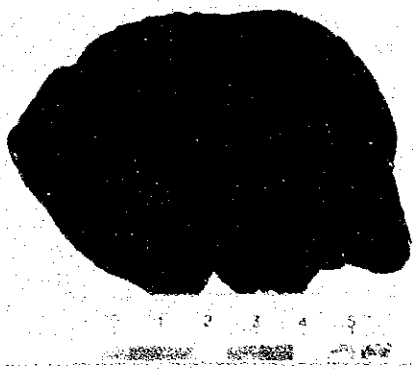
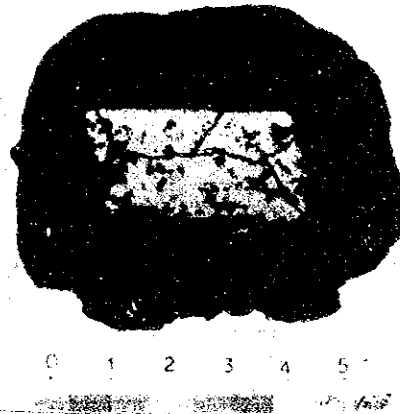


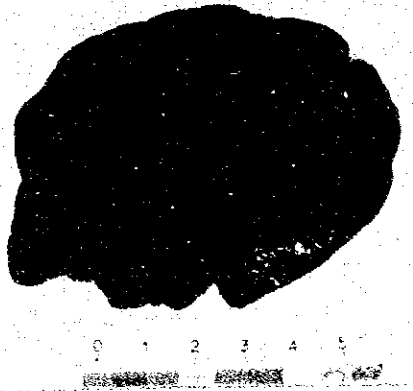
Figure 3-5-3 Morphology of Manganese Nodules (2)



Upper surface

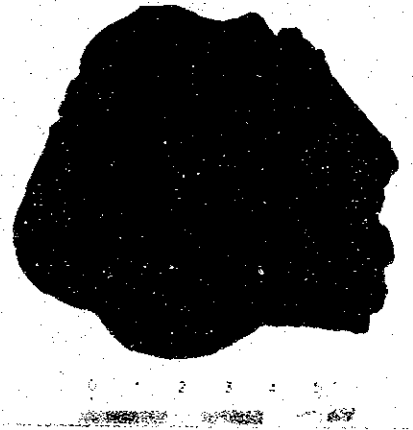


Section

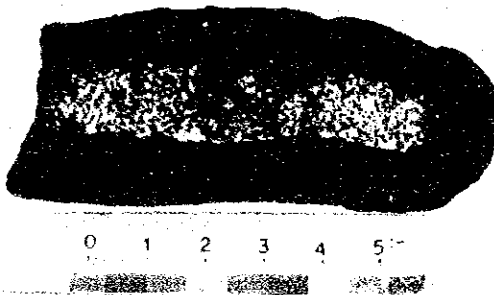


Bottom

Massive type
89S1341FG02

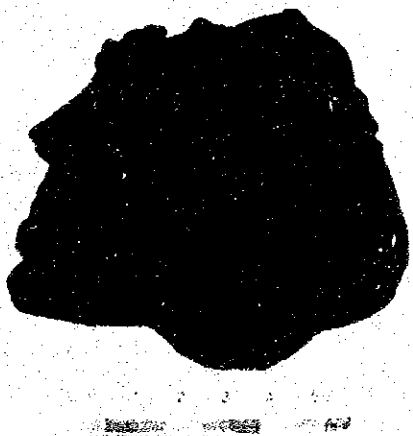


Upper surface



Section

Plate type
89S1341FG03



Bottom

Figure 3-5-3 Morphology of Manganese Nodules (3)

